2016

Mapping the Substrate of Atrial Fibrillation: Tools and Techniques

Bryce Eric Benson
University of Vermont

Mapping the Substrate of Atrial Fibrillation: Tools and Techniques

A Dissertation Presented

by

Bryce E. Benson

to

The Faculty of the Graduate College

of

The University of Vermont

In Partial Fulfillment of the Requirements
for the Degree of Doctor of Philosophy
Specializing in Bioengineering

October, 2016

Defense Date: August 25th, 2016
Dissertation Examination Committee:

Peter Spector, M.D., Advisor
Jason Bates, Ph.D.
Mary Dunlop, Ph.D.
Margaret Eppstein, Ph.D., Chairperson
Cynthia J. Forehand, Ph.D., Dean of Graduate College

Abstract

Atrial fibrillation (AF) is the most common cardiac arrhythmia that affects an estimated 33.5 million people worldwide. Despite its prevalence and economic burden, treatments remain relatively ineffective. Interventional treatments using catheter ablation have shown more success in cure rates than pharmacologic methods for AF. However, success rates diminish drastically in patients with more advanced forms of the disease.

The focus of this research is to develop a mapping strategy to improve the success of ablation. To achieve this goal, I used a computational model of excitation in order to simulate atrial fibrillation and evaluate mapping strategies that could guide ablation. I first propose a substrate guided mapping strategy to allow patient-specific treatment rather than a one size fits all approach. Ablation guided by this method reduced AF episode durations compared to baseline durations and an equal amount of random ablation in computational simulations. Because the accuracy of electrogram mapping is dependent upon catheter-tissue contact, I then provide a method to identify the distance between the electrode recording sites and the tissue surface using only the electrogram signal. The algorithm was validated both *in silico* and *in vivo*. Finally, I develop a classification algorithm for the identification of activation patterns using simultaneous, multi-site electrode recordings to aid in the development of an appropriate ablation strategy during AF.

These findings provide a framework for future mapping and ablation studies in humans and assist in the development of individualized ablation strategies for patients with higher disease burden.

Citations

Material from this dissertation has been published or is in preparation in the following form:

Benson, B.E., Carrick, R.T., Habel, N., Bates, O.R.J., Bates, J.H.T., Bielau, P., Spector, P.S.. (2014). Mapping Multi-Wavelet Reentry without Isochrones: An Electrogram-Guided Approach to Define Substrate Distribution. Europace, 16, 102-109.

Benson, B.E., Carrick, R.T., Habel, N., Bates, J.H.T., Spector, P.S.. Mapping Multi-Wavelet Reentry: An Electrogram Derived Metric to Identify Tissue Contact. Circulation: Arrhythmia and Electrophysiology.

Benson, B.E., Carrick, R.T., Bates, J.H.T., Spector, P.S.. Neural Network for Real-Time Classification of Activation Patterns in Atrial Fibrillation. Journal of Computational Biology.

Acknowledgements

The pursuit of my doctorate degree has been a fantastic, and sometimes stressful, experience that would not have been possible without the support of advisors, friends, and family. I would like to use this time to acknowledge some of these people who have made my time here possible. Firstly, thank you to my parents, Mark and Bonnie, who have not only provided their love and encouragement, but also a stress-free and warm environment to come home to. Thank you to my brothers, Patrick and Kirk, for always believing in me and being excellent role models and friends. To my future sister-in-law, Lyndsey, thank you for being the sister I never had and providing laughter throughout this experience. Thank you to my research advisor Peter Spector for the incredible opportunity and scientific support along the way. Thank you to my academic advisor Jason Bates for keeping me on track while providing seemingly endless engineering expertise. Thank you to my fellow researchers, Philipp, Nici, and Rick for making me feel less guilty about eating pizza every day and for their friendship and guidance throughout this process. Thank you to Gabby and Charlie for being there for me every step of the way to keep my mind clear of stress. Finally, thank you to my dogs, Loki and Rue, who still put up with me despite my constant need to cuddle them.

Table of Contents

List of Figures

List of Tables

Chapter 1

Introduction

The cardiovascular system is a closed system of tubes responsible for providing nutrients and oxygen to the body while removing wastes. These critical functions are mediated by the continuous circulation of blood pumped by the heart. Fundamentally, the mechanism of the heart is a simple pulsatile flow pump in which its contents are ejected at regular intervals. However, this mechanical function is the result of the coordinated contraction of the building blocks of the heart, cardiac myocytes. Individually, myocytes behave without direct neural control but rather initiate a contraction, or action potential, when neighboring myocytes pass a sufficient amount of current to exceed a threshold voltage. This, in turn, initiates action potentials in its neighbors via voltage gradients. Therefore, a single contraction of the heart is the result of a wave of electrical excitation passing from cell to cell until all cells become excited and contract as a cohesive whole.

We can think of the heart as a complex system. As such, depending on the properties and initial conditions of its building blocks, a number of different emergent behaviors may manifest. In a normal heart beat, pacemaker cells in the superior right atrium initiate a wave of excitation that propagates in a serial pattern through the atria and extinguishes at the inferior left atrium. Ventricular myocytes become excited via multiple insertion points, known as the Purkinje fibers, via activation

of the atrioventricular node which results in a coordinated ventricular contraction. Therefore, a single activation of the pacemaker cells leads to the excitation of all cardiac myocytes followed by quiescence until the following paced beat begins.

Given a different set of initial conditions, such as a premature atrial contraction, a pathological arrhythmia can be created. One such behavior, known as reentry, consists of a single wave of excitation that continues to re-excite myocytes via rotational motion. This motion may be around a structural obstacle such as a valve or a fixed point. In this case, the rate of the heart is dependent on the cycle length around the point or obstacle rather than enervated pacemaker cells. If the reentry remains spatially stable, this arrhythmia is known as tachycardia. Similar to a normal heart beat, tachycardia follows a predictable pattern of excitation but does not require re-initiation. Further modulation of the electrical properties and heterogeneity between building blocks can create a more chaotic diseased state. Similar to tachycardia, fibrillation is a reentrant arrhythmia whose rate is independent of pacemaker cells in the right atrium. However, fibrillation lacks a repeating pattern of activation and can be described by spatially and temporally unstable spiraling waves causing unsynchronized contraction of the muscle fibers in the heart. Atrial fibrillation is regarded as the most common sustained arrhythmia and has been the topic of research for scientists and physicians over the past 500 years.

Evidence of atrial fibrillation was first acknowledged by physicians in ancient Chinese, Egyptian, and Greek civilizations via a chaotic irregular arterial pulse thousands of years ago [1]. While a number of scientists were able to witness chaotic contractions in the atria as early as the 1600's [2], insights into the pathophysiology of atrial fibrillation would not come until the early 1900's when a number of technological

advances allowed observational measurements of the heart. James Mackenzie was the first scientist to make direct measurements of the human pulse with the kymograph and observed the irregularly timed beats during atrial fibrillation [3]. However, it was the development of the electrocardiogram in the early 1900's that created a much larger interest in the field of atrial fibrillation. Since its development, the number of published papers about atrial fibrillation have increased exponentially. Electrograms provided the ability to observe the electric potential field generated by myocytes such that they could track the motion of conduction throughout the tissue. This allowed physicians to identify the mechanism for sinus rhythm and a number of simple arrhythmias.

Despite the advancements of electrocardiography to be able to observe electrical conduction in the heart, a consensus for the mechanism of atrial fibrillation could not be reached. Early observations by Sir Thomas Lewis suggested that reentry was the cause for the perpetuation of atrial fibrillation [4]. Following stimulation of the atrial appendage until sustained fibrillation was achieved, he then separated the appendage from the rest of the atria. After its removal, fibrillation stopped in the appendage but continued in the remainder of the tissue. He therefore deduced that reentry must be the mechanism behind sustained fibrillation because no additional current was being added. He also proposed that a critical tissue mass is required to support the perpetuation of fibrillation as a result of the rapid termination of fibrillation in the appendage following removal from the atria.

Observations by Scherf [5] in canine atria led to the theory that atrial fibrillation was driven by ectopic foci. Injection of aconitine caused rapid excitation of a region of tissue and led to changing activation sequences in regions distal from the

focally firing tissue. After he removed the focal firing via cooling of the tissue and the arrhythmia stopped, he was led to believe that fibrillation was the result of islands of refractory tissue causing a changing activation pattern from the focal firing region. These findings were refuted by Gordon Moe [6] who repeated a similar experiment to both Scherf and Lewis by inducing atrial fibrillation via burst pacing in the atrial appendage. He then clamped off the appendage from the rest of the atria and stopped pacing. This produced a similar result to Sir Thomas Lewis, with fibrillation ceasing in the clamped off appendage but continuing in the rest of the atria. Moe proposed perpetuation was likely due to a number of reentrant wavelets acting independently causing the chaotic electrocardiograms and coined the term multiple wavelet hypothesis to describe this phenomenon [7].

More recently, scientists have developed advanced computational models to mimic the behavior of cardiac myocytes in order to study atrial fibrillation with complete control over the parameter space. The Courtemanche model [8] is a widely used model that allows control of individual ion channels making it useful for both studying the mechanism of the disease as well as drug interactions to improve pharmacological treatments. Directly observing the chaotic rhythms produced in computational models under a range of different parameters prove that both reentry and rhythms driven by ectopic foci can act as the driving force for atrial fibrillation.

Despite a number of theories describing the mechanism of atrial fibrillation and complete observation of the disease using computer models, treatments have not had nearly the same success as other reentrant arrhythmias. This is likely in part due to the progressive nature of the disease. The longer the heart continues to fibrillate, properties of the individual myocytes change to support fibrillation further. The size

of the atria also grows due to its perpetual use during fibrillation. Pharmacologic treatments attempt to reverse some of these effects on the tissue substrate to prevent atrial fibrillation from perpetuating, but alone have shown limited success in patients with advanced forms of atrial fibrillation. An early surgical treatment, known as the MAZE procedure [9, 10, 11, 12, 13, 14], acted on the findings of the critical mass hypothesis to section the atria into smaller electrically divided regions. While this method showed a high success rate, the procedure required an open chest to perform and is usually only performed as an add-on during other cardiovascular surgeries. Endocardial catheter ablation therapy allowed the electrical isolation techniques to be achieved with a minimally invasive approach. The most common method for ablation today involves the isolation of the pulmonary veins from the rest of the atria as a means of removing sources of ectopic foci [15]. This procedure has a high rate of success for early onset cases but success rates diminish for advanced forms of atrial fibrillation. More recent approaches such as CFAE ablation [16], which targets areas of tissue that generate complex electrograms, and FIRM mapping [17], which identifies spiral wave drivers, have taken a more targeted approach for when traditional ablation is insufficient but nothing has been able to match the success rates achieved in other arrhythmias.

The primary goal of this thesis is to develop a mapping strategy for the successful ablation of atrial fibrillation. To achieve this, I used a computational model of excitation that sacrifices some of the intricacies seen in the Courtemanche model to achieve a high throughput in order to study the wide range of parameter values seen during the progression of atrial fibrillation. I propose a substrate guided mapping strategy to treat a specific arrhythmia rather than a one size fits all approach. To improve this

method, I then provide an electrogram derived metric for improved electrode spatial resolution. Finally, I develop a method for classification of local activation patterns using simultaneous, multisite electrode recordings to assist in ablation strategies.

Bibliography

[1] Peter M Dunn. "Maimonides (1135-1204) and his philosophy of medicine". In: *Archives of Disease in Childhood - Fetal and Neonatal Edition* 79.3 (1998), F227.

[2] T. Fazekas. "[The concise history of atrial fibrillation]". In: *Orvostort Kozl* 53.3-4 (2007), pp. 37–68.

[3] J. Mackenzie. "The Interpretation of the Pulsations in the Jugular Veins." In: *Am J Med Sci* 134 (1907), pp. 12–34.

[4] Joel Howell. "Two pioneers of electrocardiography. The correspondence between Einthoven and Lewis from 1908-1925". In: *Medical History* 29.2 (1985), pp. 224–225.

[5] D. Scherf, F. J. Romano, and R. Terranova. "Experimental studies on auricular flutter and auricular fibrillation". In: *Am Heart J* 36.2 (1948), pp. 241–251.

[6] G. K. Moe and J. A. Abildskov. "Atrial fibrillation as a self-sustaining arrhythmia independent of focal discharge". In: *Am Heart J* 58.1 (1959), pp. 59–70.

[7] Gordon K. Moe, Werner C. Rheinboldt, and J. A. Abildskov. "A computer model of atrial fibrillation". In: *Am Heart J* 67.2 (1964), pp. 200–220.

[8] M. Courtemanche, R. J. Ramirez, and S. Nattel. "Ionic targets for drug therapy and atrial fibrillation-induced electrical remodeling: insights from a mathematical model". In: *Cardiovasc Res* 42.2 (1999), pp. 477–89.

[9] J. L. Cox et al. "Current status of the Maze procedure for the treatment of atrial fibrillation". In: *Semin Thorac Cardiovasc Surg* 12.1 (2000), pp. 15–9.

[10] J. L. Cox et al. "Five-year experience with the maze procedure for atrial fibrillation". In: *Ann Thorac Surg* 56.4 (1993), pp. 814–823, 814–823.

[11] J. L. Cox et al. "The surgical treatment of atrial fibrillation. II. Intraoperative electrophysiologic mapping and description of the electrophysiologic basis of atrial flutter and atrial fibrillation". In: *J Thorac Cardiovasc Surg* 101.3 (1991), pp. 406–26.

[12] J. L. Cox, R. B. Schuessler, and J. P. Boineau. "The surgical treatment of atrial fibrillation. I. Summary of the current concepts of the mechanisms of atrial flutter and atrial fibrillation". In: *J Thorac Cardiovasc Surg* 101.3 (1991), pp. 402–5.

[13] J. L. Cox et al. “Surgery for atrial fibrillation”. In: *Semin Thorac Cardiovasc Surg* 1.1 (1989), pp. 67–73.

[14] J. L. Cox et al. “The surgical treatment of atrial fibrillation. III. Development of a definitive surgical procedure”. In: *J Thorac Cardiovasc Surg* 101.4 (1991), pp. 569–83.

[15] M. Haissaguerre et al. “Catheter ablation of long-lasting persistent atrial fibrillation: critical structures for termination”. In: *J Cardiovasc Electrophysiol* 16.11 (2005), pp. 1125–37.

[16] Sanjay Dixit et al. “Randomized Ablation Strategies for the Treatment of Persistent Atrial Fibrillation: RASTA Study”. In: *Circulation: Arrhythmia and Electrophysiology* 5.2 (2012), pp. 287–294.

[17] Sanjiv M. Narayan, David E. Krummen, and Wouter-Jan Rappel. “Clinical Mapping Approach To Diagnose Electrical Rotors and Focal Impulse Sources for Human Atrial Fibrillation”. In: *J Cardiovasc Electrophysiol* 23.5 (2012), pp. 447–454.

Chapter 2

Literature Review

2.1 Cardiac Electrophysiology

2.1.1 Basics of Cardiovascular Physiology

The primary function of the heart is to distribute blood throughout the body. More specifically, the heart can be described as two separate pumps. The right side of the heart receives deoxygenated blood that has circulated through the body and sends it to the lungs to be oxygenated. Oxygenated blood then returns to the left side of the heart to be pumped out through the body again. Each side of the heart can be further subdivided into top and bottom halves, known as atria and ventricles, respectively. The atria passively collect blood returning to the heart from the veins and fill the ventricles. The ventricles are much larger chambers with thicker walls allowing sufficient force to deliver blood to the body or lungs. Atria and ventricles are separated by unidirectional valves to keep the blood from regurgitating back into the atria as well as fibrous tissue which, unlike the rest of cardiac tissue, acts as an electrical insulator effectively separating the top and bottom heart.

The mechanical behavior of the heart is contingent on its electrical conduction system. When sufficient ionic current reaches the membrane of a cardiac muscle cell

to increase its membrane potential beyond a threshold, it undergoes a pattern of excitation known as an action potential. When this occurs, membrane permeability to ions drastically changes causing a rapid depolarization of the transmembrane potential. This also triggers the release of intracellular calcium and the initiation of a mechanical contraction. The depolarized cell passively exchanges current with its neighboring cells due to electrochemical gradients which can lead to its action potential when the membrane potential exceeds a threshold. Importantly, cells that have been recently excited enter a period of refractoriness when it cannot undergo an additional action potential until its potential repolarizes towards its resting potential. This causes excitation to propagate unidirectional throughout the tissue and leads to the simultaneous contraction of multiple myocytes.

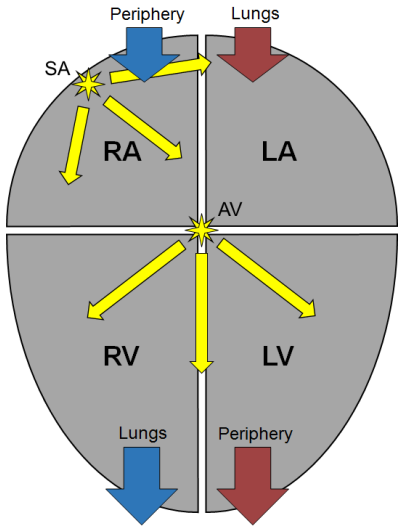

Figure 2.1: Simplified schematic of the four chambers of the heart: Right atrium, left atrium, right ventricle, and left ventricle (RA, LA, RV, LV respectively) showing both electrical conduction pathways (yellow) and blood flow (red and blue). Electrical conduction begins in the sinus node (SA) and passes to the ventricles via the atrioventricular node (AV).

In a healthy normally functioning heart, excitation begins in the superior right atrium with a group of cells capable of spontaneous depolarization. This group of cells, known as the sinoatrial (SA) node, determine the heart rate and are highly regulated by the parasympathetic nervous system. Conduction through the atria spreads in a serial pattern causing each cell to become excited once per activation of the SA node. Excitation from the atria passes to the ventricles via the atrioventricular (AV) node. The AV node contains cells with fewer intercellular ion channels that act to delay the conduction time between the atria and ventricles. This delay allows the ventricles to become filled with blood before initiating a contraction. From the AV node, conduction passes through a network of fibers with widely distributed ventricular access points. Therefore, electrical conduction begins at multiple insertion points in the ventricles causing a parallel excitation pattern and a more coordinated contraction.

2.1.2 Atrial Fibrillation

Atrial fibrillation (AF) is the most common cardiac arrhythmia, or irregular rhythm, affecting an estimated 33.5 million people worldwide [1]. It can be described as a disorganized and highly irregular electrical conduction pattern through the atrial tissue. Mechanically, this manifests as a quivering motion, preventing the upper chambers of the heart to act as an effective pump to fill the ventricles. Fortunately, the majority of ventricular filling is a passive process and therefore the mechanical dysfunction of the atria is not a large burden on the cardiac output. The mechanical function of the ventricles is largely unaffected by the chaotic rhythm occurring in the atria, but contractions occur at intermittent rates due to the excitation

of the AV node at irregular intervals. This can typically be observed clinically via an electrocardiogram (EKG) by irregularly timed QRS complexes with little evidence of a P-wave.

Although episodes of atrial fibrillation are not considered to be deadly, AF is associated with an increased risk of a number of life-threatening outcomes. Cardioembolic stroke is frequently observed in patients suffering from AF due to the mechanical failure of the atria. Because AF causes the atria to act ineffectively as a pump, blood can become stagnant and coagulate over time. This coagulation, or thrombus, can then become a blockage downstream. Extended episodes of atrial fibrillation may also cause cardiomyopathy due tachycardia over a long period of time. If left untreated, this can lead to heart failure. While not all patients are symptomatic experiencing an episode of AF, common symptoms include weakness, dizziness, and fatigue. Each of the above complications leads to a decreased quality and life and an estimated two-fold increased risk of mortality [2].

Over the past ten years, there has a been a rise in both the incidence and prevalence of atrial fibrillation [1, 3, 2]. Incidence and prevalence of AF are expected to increase substantially over the next 20 years [4] due to increased screening as well as a growing older population with underlying heart abnormalities such as heart disease [5, 6, 7, 8, 9]. AF is more commonly observed in men than women (1.1% to 0.8% overall) and this difference in observed in all age groups [6]. The high incidence and morbidity of AF and its associated diseases impose a significant financial burden. Costs of healthcare for patients with AF in the United States alone are estimated to be $6.5 billion per year [10].

The severity of atrial fibrillation can be classified by the proportion of time spent

in AF. The most recent guidelines classify the severity of AF into four categories: paroxysmal, persistent, long-standing persistent, and permanent[11, 12, 13, 14, 15]. Paroxysmal AF describes short duration episodes with spontaneous termination and variable reoccurrence. Episodes of AF lasting longer than seven days that typically require some form of intervention are classified as Persistent AF. Long-standing persistent AF is defined by episodes that last longer than 12 months. Finally, Permanent AF is used to describe patients with irreversible episodes of fibrillation. Furthermore, atrial fibrillation is a progressive disease; if left untreated, the rate of progression from paroxysmal AF to persistent and/or permanent AF is reported to be 25% of patients within five years [16, 17, 18]. During extended exposure to episodes of fibrillation, changes occur in the atrial substrate, known as remodeling, allowing the tissue to more easily support future occurrences of AF [19, 20]. Unfortunately, treatment success rates diminish drastically for advanced forms of atrial fibrillation [14] implying the importance for both early detection and treatment of AF.

2.2 Mechanisms of Atrial Fibrillation

In order to develop an effective strategy for the treatment of atrial fibrillation, the mechanism for its perpetuation should be investigated. While scientists and physicians were able to observe irregularly timed ventricular contractions and fibrillating tissue several centuries ago [21, 22, 23], concrete theories regarding the perpetuation of AF would not surface until the development of electrocardiography provided our modern understanding of electrophysiology. With the help of intracardiac electrograms and later development of computer models to simulate the behavior of atrial

fibrillation, two leading theories emerged to describe its mechanism: *multi-wavelet reentry* and *focal drivers with fibrillatory conduction*. Regardless of which theory governs the mechanism of atrial fibrillation in the majority of patients, all would agree that ongoing fibrillation requires a continuous source electrical activity. There are two distinct mechanisms by which tissue is supplied with continuous electrical activity. First, spontaneous depolarization in the atria can occur frequently enough to outpace the sinus node. The disorganized activity commonly witnessed in AF is then produced when spontaneously formed wave fronts encounter refractory tissue which causes the wave to divide and conduct in irregular pathways. This irregular wave pattern caused by a focal source is known as fibrillatory conduction.

Secondly, a wave whose path progresses in an uninterrupted circular motion can propagate indefinitely. So long as the conduction time to complete a revolution exceeds the repolarization time of local cells, the wave front will always encounter excitable tissue. The circular path, or circuit, that a wave travels can be either spatially stable or dynamic. The first case, known as a focal rotor, mechanistically behaves similarly to ectopic foci acting as a stable source of electrical activity. The stable source can then cause fibrillatory conduction in regions of tissue with insufficient repolarization time to compete with the source activation rate. Dynamic reentrant circuits frequently interact with refractory tissue causing wave break and spawning daughter wavelets. These daughter waves can then form circuits of their own contributing to the perpetuation of AF. The chaotic interactions between multiple dynamic reentrant waves are commonly known as multi-wavelet reentry (MWR). Over the past 100 years, evidence for both focal sources as well as multi-wavelet reentry has been presented. While both theories are theoretically feasible and have been demonstrated

in computer models, successful treatment is contingent on identifying the governing mechanism behind atrial fibrillation.

2.2.1 Evidence of Multi-Wavelet Reentry

Early observations of atrial fibrillation in a canine atria by Moe [24] suggested that the perpetuation of AF was caused by the wandering of multiple wavelets continuously re-exciting non-refractory tissue. These findings formed the basis for the multiple wavelet hypothesis, later termed multi-wavelet reentry (MWR). This theory agreed with earlier observations by Garrey [25] suggesting that fibrillation required a critical mass in order to perpetuate. Following continuous stimulation in the atrial appendix to induce fibrillation, the appendix of the tissue was removed. Irregular conduction continued in the atria while fibrillation in the appendix terminated when stimulation was removed. Moe later demonstrated the feasibility of MWR in the development of a computer model of cardiac propagation [26]. Additionally, Moe expanded on the critical mass hypothesis proposed by Garrey suggesting that the minimal area of tissue was not a constant value but rather a measure of the size of wavelets in the tissue.

Simultaneous, multi-site electrogram recordings allowed higher resolution mapping to investigate activation patterns during atrial fibrillation. A study of canine heart with acetylcholine-induced AF by Allessie [27] with 192 simultaneously recorded electrograms showed beat to beat changing activation patterns. He concluded the critical number of wavelets in the left and right atria required to maintain AF was between three and six. Konings [28] later performed high-density mapping of AF in humans with Wolff-Parkinson-White syndrome. The degree of disorganization observed in the

atria was related to the frequency of atrial fibrillation. In the most chronic cases of AF observed, random reentrant waves were frequently observed. Multiple wavelets were further identified by other groups using multisite electrode mapping [29, 30].

2.2.2 Evidence of Focal Drivers

Prior to Moe's postulation of the multiple wavelet hypothesis, Scherf [31] suggested fibrillation was initiated and perpetuated by rapid ectopic beats. Injection of aconitine in canine atria caused rapid impulse formation with disorganized fibrillation away from the source. After tissue cooling, the impulse formation stopped as well as the fibrillation. When cooling was interrupted, the ectopic foci reappeared and fibrillation continued. While many argue that this fibrillation was induced by an artificial substrate because aconitine induces focal firing, ectopic beats were later observed in future studies [32, 33, 34]. These findings were supported by future multi-site electrode mapping studies with basket catheters by Narayan [35, 36]. Using unipolar electrode recordings, activation maps identified both ectopic beats as well as focal rotors.

An alternative to multi-site electrode arrays for activation pattern detection is optical mapping. Via injection of a voltage sensitive dye, cells emit a visible wavelength of light during activation. Using this technique, Jalife [37] induced atrial fibrillation in sheep hearts and identified focal rotor sites. He concluded that multiple wavelets observed were the result of breakup caused by higher frequency organized rotors and could not be the mechanism for AF alone. This was tested in a separate study in which Jalife used spectral analysis of bipolar electrograms collected in humans during atrial fibrillation [38]. In 32 patients with paroxysmal and permanent atrial fibrilla-

tion, the dominant frequency and its 1:1 conduction zone were shown to be responsible for AF maintenance. When these sites were removed, fibrillation terminated in 87% of patients. The remain patients showed a significant slowing of the frequency of AF.

Substantial evidence has been presented in support of both focal drivers with fibrillatory conduction as well a multi-wavelet reentry. The breadth of sometimes contradictory results can be contributed to a number of different factors. First, the models used to study atrial fibrillation are not consistent among studies. It is plausible that canine atria have a structural substrate better suited to support focal rotors or ectopic foci than the atria of a sheep. Also, physiologic responses to drugs are likely to be variable among different species. Secondly, it is widely known that atrial fibrillation is a progressive disease. Patients with lower disease burden (paroxysmal AF) will have different structural and functional substrate than someone with permanent atrial fibrillation. As such, it is likely that the mechanism for the maintenance of AF is dependent on the severity of disease burden. The lack of agreement on the mechanism for AF is reflected by our failure to develop an adequate strategy for its treatment.

2.3 Treatments for Atrial Fibrillation

Despite the economic and clinical burden imposed by atrial fibrillation, treatment options remain limited. While success rates for other cardiac arrhythmias such as atrial flutter are well above 95%, even aggressive treatment options for atrial fibrillation fail to achieve success rates above 75% in patients with paroxysmal AF [39]. Treatments for AF can be divided into two main categories: pharmacological and interventional.

2.3.1 Pharmacological Treatments

Pharmacologic therapy can be further subdivided into two major groups to treat the symptoms of AF: rate control and rhythm control drugs. Anti-arrhythmic therapy for younger patients or those who are highly symptomatic is typically directed toward a rhythm control strategy. The goal of this therapy is the maintenance of sinus rhythm in order to achieve a higher quality of life [40]. To achieve this, rhythm control drugs modify the atrial tissue substrate to reduce its propensity to initiate and support future episodes of atrial fibrillation. Drugs commonly used for rhythm control strategies either interfere with sodium channels (Quinidine and Flecainide) or block potassium channels (Amiodarone and Dofetilide) [41]. On the other hand, rate control therapy aims to control the ventricular rate rather than the maintenance of sinus rhythm. These drugs target cells in the AV node that are responsible for transferring conduction between the atria and ventricles. Rate control is achieved by either slowing or blocking the irregular patterns of conduction reaching the AV node from the fibrillating atria. Rate control drugs are typically divided into two categories: beta blockers (propranolol and metoprolol) and calcium channel blockers (verapamil and diltiazem) which both act by decreasing conduction through the AV node [41].

Despite the widespread use of pharmacologic treatments for atrial fibrillation, rate control and rhythm control drugs have shown marginal success in clinical trials. In the AFFIRM trial (n = 2,027), rate control was achieved in 58% of patients while sinus rhythm was maintained in approximately 52% of patients [39, 42]. While rhythm control drugs are desirable for their ability to maintain sinus rhythm and

eliminate fibrillation, further analyses have shown a positive trend toward increasing mortality rates due to a higher risk of complications associated with the medications [42]. Furthermore, patients on both rate and rhythm control therapy are typically put on anti-thrombotic therapy to reduce the likelihood of stroke [43].

2.3.2 Interventional Treatments

While anti-arrhythmic therapies attempt to manage atrial fibrillation through alteration of cellular properties, interventional methods modify the architecture of the heart in order to reduce the likelihood of AF perpetuation and initiation. The earliest interventional treatment to show high rates of success in curing AF was the surgical Maze procedure introduced by Cox [44, 45, 46, 47]. Applying the findings of early physiologists that the maintenance of AF required a critical mass of tissue [25], the Maze procedure involves a series of transmural incisions producing a maze-like pattern in the atria limiting the tissue's ability to support macro-reentry. Since its introduction, the success rate of freedom from AF is reported to be 98% [48, 49]. However, due to the complexity of the surgery as well as the requirement of a cardiopulmonary bypass for an arrested heart, most physicians and patients opt for other treatments [50]. The introduction of more minimally invasive interventional methods has further relegated the Maze procedure to patients requiring other open chest procedures such as valve repairs to be done concurrently or patients with an extremely high disease burden.

Since the 1960's, physicians and scientists have used minimally invasive methods to gain access to the heart for both mapping and stimulation [51]. This is achieved by threading an electrode-tipped catheter through the venous system. Catheter-based

ablation, introduced in the 1990's, enabled the formation of electrically unexcitable scars by applying radiofrequency (high frequency) current to the cardiac tissue causing resistive heating [52]. However, unlike surgical methods, incomplete radiofrequency ablation may temporarily inhibit the ability of cells to electrically conduct rather than cause permanent scars [53, 54]. This results in a high incidence of repeat ablation procedures to correct incomplete lesions [55]. Despite the risk of repeat procedures and difficulty to achieve accurate and complete lesions in an actively beating heart, catheter ablation has been the most widely accepted interventional treatment for AF over the past 20 years.

A number of strategies for catheter-based ablation have evolved since its introduction. However, the most common ablation strategy evolved via the recognition of ectopic foci in the pulmonary veins [32]. These foci were identified as precursors to episodes of AF. As a result, ablation lesions are placed circumferentially around the pulmonary veins to isolate them from the atria. This method, known as pulmonary vein isolation (PVI) has shown moderate success in patients with paroxysmal AF by eliminating episodes at one-year follow-up in 62-87% of patients [39, 56, 57, 58]. Success rates of PVI for patients with persistent atrial fibrillation are significantly lower with single procedure success rates below 50% and multiple procedure rates around 60% [56, 57, 58, 59, 60].

Due to the variable success of PVI to treat patients with persistent AF, a number of additional linear lesions have been proposed on top of traditional PVI in order to compartmentalize the atria and prevent macro-reentry similar to the Maze procedure. The most commonly applied additional lesions are the roof line, mitral isthmus line, and cavotricuspid isthmus line (shown in Figure 2.2). Each of these additional lines

has shown success over PVI alone; however, none have shown the same success rates as the Maze procedure. In paroxysmal AF patients, success rates were 69% with PVI alone versus 87% with the placement of addition lesions [61]. Success rates in persistent AF improved from 39% to 75% with the placement of additional lesions [56, 57, 59, 60].

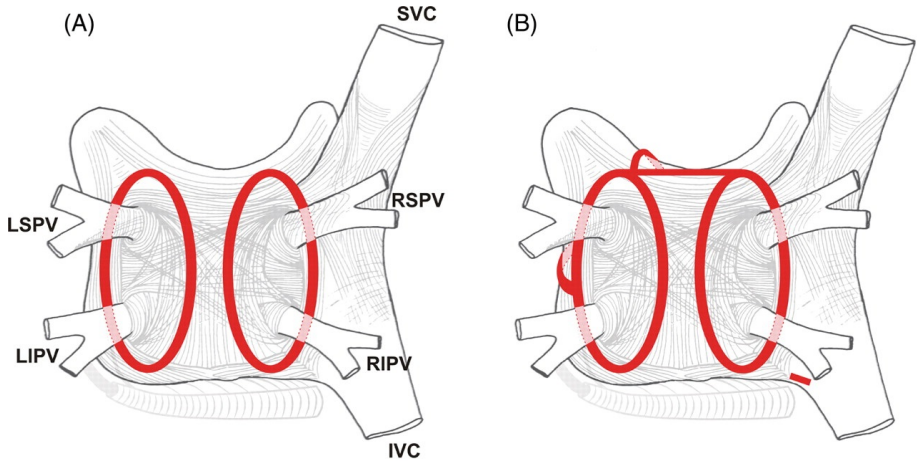

Figure 2.2: Posterior view of left and right atria of common lesion sets employed for AF ablation. (A) Pulmonary vein isolation lesion set; LSPV, LIPV, RSPV, and RIPV refer to the left and right superior and inferior veins. SVC and IVC refer to the superior and inferior vena cava. (B) Traditional pulmonary vein isolation with additional roof line, mitral isthmus line, and cavotricuspid isthmus line. Modified from Calkins et al. [14]Posterior view of left and right atria of common lesion sets employed for AF ablation.

Each of the previously described strategies for interventional treatment of atrial fibrillation utilized a blind, one-size-fits-all approach. While this showed significant success in the Maze procedure, more recent catheter-based ablation strategies have failed to emulate the same results especially in patients with high disease burden. Unlike arrhythmias such as atrial flutter in which there is a repeating sequence of activation, atrial fibrillation not only varies over time, but also between patients

depending on the structural and functional substrate it is presented. As a result, one region of tissue acting as a driving force for AF in an individual patient may be completely different than another. One of the main benefits to catheter-based ablation is its ability to simultaneously record the intracardiac potentials to identify potentially advantageous sites for ablation.

In an early mapping study, the morphology of unipolar electrograms in various locations throughout the atria during AF was correlated with varying patterns of activation [62]. The most complicated electrogram morphology, termed fragmented potentials, were associated with slow conduction regions or pivot points of activation. Acting on these findings, Nademanee et al. [63] argued that these sites, which he called complex fractionated atrial electrograms (CFAEs), could serve as target sites for focal catheter ablation of AF. In his original study of 121 patients with equal rates of paroxysmal and persistent AF, ablation of CFAE sites resulted in the termination of AF in 95% of patients and 91% free of AF at one-year follow-up.

While the original CFAE ablation trial showed high success rates in both paroxysmal and persistent cases of AF, future studies failed to achieve repeatable results in either paroxysmal and persistent AF patients [64, 65, 66, 67, 68, 69, 70, 71, 72, 73]. The majority of studies investigated the benefit of adding CFAE ablation to the standard pulmonary vein isolation. Of these, only two suggested CFAE ablation improved outcomes over PVI alone. One of the biggest arguments regarding CFAEs is the lack of a universal definition. The studies presented utilized multiple detection algorithms or visual inspection to identify fractionated sites. Perhaps more importantly, a fractionated electrogram can be produced by a variety of different activation patterns such as conduction slowing, wave collision, and the combined potential field

resulting from two dissociated waves. Each of these factors has contributed to CFAE ablation becoming less favorable within the electrophysiology community.

In an optical mapping study with Langendorff sheep hearts, the Jalife group identified multiple spatially stable high-frequency rotors. Dissociated regions of tissue were also observed in the optical maps; however, the frequency of activation in these regions was lower suggesting they were being driven by the higher frequency drivers [38]. Because the rotors identified were spatially stable, the cycle lengths between activations are temporally consistent. Using a Fourier transform to decompose the recorded electrograms into their component frequencies, rotor sites could be easily identified by a prominent, and high magnitude, peak in the frequency histogram known as the dominant frequency (DF) [74]. Using this spectral analysis technique, the Jalife group mapped atrial fibrillation in both paroxysmal and permanent AF in humans. In patients with paroxysmal atrial fibrillation, DF sites were most commonly observed in the pulmonary veins (11 out of 13). Dominant frequency sites were much more prevalent around the atria in permanent AF. Following ablation of the identified DF sites, AF terminated in 87% of paroxysmal cases. Ablation of DF sites in patients with permanent AF had no effect (0 out of 13).

Further studies using DF mapping showed similar results [75] resulting in some success treating patients with low disease burden but failing to effectively treat persistent and permanent AF. Failure of termination in patients with persistent arrhythmia may have been due to a number of factors. First, ablation did not include all the critical focal drivers responsible for its maintenance. Second, DF sites were not identified due to insufficient frequency gradients between focal sources and passively fibrillating tissue. Third, the mechanism for AF maintenance is fundamentally different in

paroxysmal versus persistent and permanent AF [38]. Due to the electrical and structural remodeling that occurs during extended episodes of AF, it is probable that a shift in the mechanism for its perpetuation was the cause for the failure of DF-guided ablation.

More recently, another mapping technique aimed at identifying focal rotors and sources has shown favorable outcomes. This technique, focal impulse and rotor modulation (FIRM), relies on unipolar electrograms from a multi-site simultaneous mapping catheter as well as repolarization dynamics from monophasic action potentials to infer activation patterns within the atria [36]. Focal sources were identified as either a rotational activation pattern (rotor) or activation radially from a point (ectopic foci). Identified focal sources are administered focal ablation [35]. Early investigations exhibited improved ablation success for FIRM guided ablation over traditional methods (82.4% vs 44.9%, respectively) after a single procedure. Follow-up investigations have shown mixed outcomes. While one study showed significant improvement over traditional ablation for treating persistent AF (80% freedom from AF) [76], another reported AF termination in only 20% of patients [77]. Several concerns arise regarding the methodology of this approach. The use of low-resolution electrodes in areas of high spatial complexity promotes the occurrence of fractionated electrograms. Also, the structure of the catheter used (128 electrode basket catheter) impedes the ability to ensure adequate contact between electrodes and the atrial tissue. Each of these aspects disrupts the accuracy of electrograms as a reflection of the true activation pattern in the atria. Ultimately, a randomized clinical trial will be required to assess the effectiveness of this approach.

2.4 Computational Models of Cardiac Excitation

One of the biggest obstacles to our understanding of the mechanism for atrial fibrillation is our inability to directly observe tissue activation during the arrhythmia. Until sampling limitations for intra-cardiac mapping of arrhythmias are overcome, computer models of excitation provide critically useful tools to study complex activation patterns with complete visibility of the system. While *in silico* models can be incredibly useful tools to form hypotheses about excitation dynamics, the usefulness of a model is limited by the assumptions on which it is based. Various levels of biological accuracy can be achieved in modeling the behavior of excitable tissue. In the most complex models, individual ion channel dynamics are modeled to study drug interactions at the extreme cost of simulation speed. On the other hand, those studying the macroscopic behavior of tissue can sacrifice some of the intricacies of biological realism to achieve high throughput models to observe long duration fibrillation events. Because the complexity of a model has a huge impact on the computational burden, the simplest model that provides insight on a hypothesis is most frequently recommended.

Generally, computational models of excitation can be divided into two categories: biophysically detailed models, which typically involve modeling intracellular dynamics with a set of ordinary differential equations, and those focused on investigating excitation propagation using rule-based models for increased computational efficacy. The majority of modern biophysical models are derived from the work of Hodgkin and

Huxley [78]. Observations of electrical behavior in the membrane of the giant squid neuron were shown to be analogous to the behavior of an electrical circuit. Earliest iterations were modeled with potassium, sodium, and leakage currents but modifications in future biophysical models expanded on this to include specific ion channel dynamics for modeling cardiac electrophysiology [79, 80, 81, 82, 83]. Because solving a set of ordinary differential equations is required to update an individual myocyte between time iterations, the computational burden to model an entire tissue of cells impedes the ability to observe propagation dynamics on the fly.

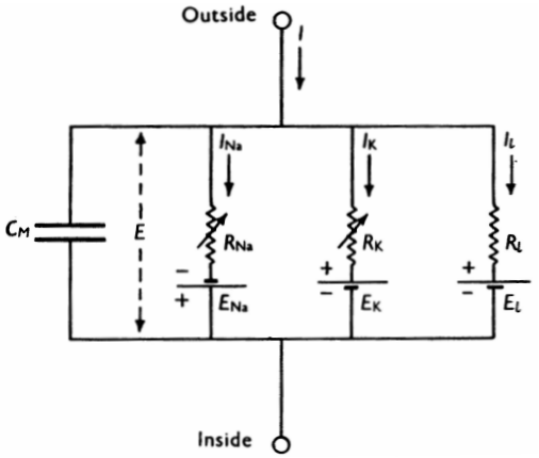

Figure 2.3: Electrical circuit representation of the giant squid neuron cell membrane. I_{Na}, I_K, and I_L correspond with sodium, potassium, and leakage current, respectively. R_{Na}, R_K, and R_L are equal to the inverse of sodium, potassium, and leakage conductance (permeability coefficient). The difference in membrane potential and equilibrium potential of ions is denoted by E. Finally, membrane capacitance is denoted by C_M. [78]

On the other hand, rule-based models such as cellular automata are favorable for rapid observation of macroscopic behavior due to changes in intercellular properties and basic electrophysiological properties like the duration of an action potential.

The earliest model of excitation by Moe [26] used to develop the multiple wavelet hypothesis was a rule-based cellular automaton. While the complexity of the model was limited by the processing power available in the 1950's, the macroscopic behavior observed was able to mimic observations seen previously in animal models of AF. A more recent iteration of rule-based models introduced by Spector and Bates [84] represents the atrial action potential as a piecewise linear model thereby eliminating the computational burden of solving a set of differential equations. Despite this simplification, complex patterns of macroscopic behavior such as rotors and multi-wavelet reentry can emerge spontaneously.

Bibliography

[1] N. J. Patel et al. "Contemporary trends of hospitalization for atrial fibrillation in the United States, 2000 through 2010: implications for healthcare planning". In: *Circulation* 129.23 (2014), pp. 2371–9.

[2] E. J. Benjamin et al. "Impact of atrial fibrillation on the risk of death: the Framingham Heart Study". In: *Circulation* 98.10 (1998), pp. 946–52.

[3] S. S. Chugh et al. "Epidemiology and natural history of atrial fibrillation: clinical implications". In: *J Am Coll Cardiol* 37.2 (2001), pp. 371–8.

[4] J. Heeringa et al. "Prevalence, incidence and lifetime risk of atrial fibrillation: the Rotterdam study". In: *Eur Heart J* 27.8 (2006), pp. 949–53.

[5] E. Svennberg et al. "Mass Screening for Untreated Atrial Fibrillation: The STROKESTOP Study". In: *Circulation* 131.25 (2015), pp. 2176–84.

[6] J. Heeringa et al. "Prevalence, incidence and lifetime risk of atrial fibrillation: the Rotterdam study". In: *Eur Heart J* 27.8 (2006), pp. 949–53.

[7] A. S. Go et al. "Prevalence of diagnosed atrial fibrillation in adults: national implications for rhythm management and stroke prevention: the AnTicoagulation and Risk Factors in Atrial Fibrillation (ATRIA) Study". In: *Jama* 285.18 (2001), pp. 2370–5.

[8] W. M. Feinberg et al. "Prevalence, age distribution, and gender of patients with atrial fibrillation. Analysis and implications". In: *Arch Intern Med* 155.5 (1995), pp. 469–73.

[9] A. Majeed, K. Moser, and K. Carroll. "Trends in the prevalence and management of atrial fibrillation in general practice in England and Wales, 1994-1998: analysis of data from the general practice research database". In: *Heart* 86.3 (2001), pp. 284–8.

[10] K. S. Coyne et al. "Assessing the direct costs of treating nonvalvular atrial fibrillation in the United States". In: *Value Health* 9.5 (2006), pp. 348–56.

[11] C. T. January et al. "2014 AHA/ACC/HRS guideline for the management of patients with atrial fibrillation: executive summary: a report of the American College of Cardiology/American Heart Association Task Force on practice guidelines and the Heart Rhythm Society". In: *Circulation* 130.23 (2014), pp. 2071–104.

[12] L. S. Wann et al. “Management of patients with atrial fibrillation (compilation of 2006 ACCF/AHA/ESC and 2011 ACCF/AHA/HRS recommendations): a report of the American College of Cardiology/American Heart Association Task Force on practice guidelines”. In: *Circulation* 127.18 (2013), pp. 1916–26.

[13] V. Fuster et al. “ACC/AHA/ESC 2006 Guidelines for the Management of Patients with Atrial Fibrillation: a report of the American College of Cardiology/American Heart Association Task Force on Practice Guidelines and the European Society of Cardiology Committee for Practice Guidelines (Writing Committee to Revise the 2001 Guidelines for the Management of Patients With Atrial Fibrillation): developed in collaboration with the European Heart Rhythm Association and the Heart Rhythm Society”. In: *Circulation* 114.7 (2006), e257–354.

[14] H. Calkins et al. “HRS/EHRA/ECAS expert Consensus Statement on catheter and surgical ablation of atrial fibrillation: recommendations for personnel, policy, procedures and follow-up. A report of the Heart Rhythm Society (HRS) Task Force on catheter and surgical ablation of atrial fibrillation”. In: *Heart Rhythm* 4.6 (2007), pp. 816–61.

[15] L. S. Wann et al. “2011 ACCF/AHA/HRS focused update on the management of patients with atrial fibrillation (Updating the 2006 Guideline): a report of the American College of Cardiology Foundation/American Heart Association Task Force on Practice Guidelines”. In: *J Am Coll Cardiol* 57.2 (2011), pp. 223–42.

[16] S. M. Al-Khatib et al. “Observations on the transition from intermittent to permanent atrial fibrillation”. In: *Am Heart J* 140.1 (2000), pp. 142–5.

[17] G. C. Flaker et al. “Clinical and echocardiographic features of intermittent atrial fibrillation that predict recurrent atrial fibrillation. Stroke Prevention in Atrial Fibrillation (SPAF) Investigators”. In: *Am J Cardiol* 76.5 (1995), pp. 355–8.

[18] C. R. Kerr et al. “Progression to chronic atrial fibrillation after the initial diagnosis of paroxysmal atrial fibrillation: results from the Canadian Registry of Atrial Fibrillation”. In: *Am Heart J* 149.3 (2005), pp. 489–96.

[19] M. C. Wijffels et al. “Atrial fibrillation begets atrial fibrillation. A study in awake chronically instrumented goats”. In: *Circulation* 92.7 (1995), pp. 1954–68.

[20] M. A. Allessie et al. “Electrophysiologic mechanisms of perpetuation of atrial fibrillation”. In: *Am J Cardiol* 77.3 (1996), 10A–23A.

[21] K.F. Wenckebach. *Arhythmia of the Heart: A Physiological and Clinical Study*. Green, 1904.

[22] W. Stokes. *The Diseases of the heart and the aorta*. Lindsay and Blakiston, 1854.

[23] Peter M Dunn. "Maimonides (1135-1204) and his philosophy of medicine". In: *Archives of Disease in Childhood - Fetal and Neonatal Edition* 79.3 (1998), F227.

[24] G. K. Moe and J. A. Abildskov. "Atrial fibrillation as a self-sustaining arrhythmia independent of focal discharge". In: *Am Heart J* 58.1 (1959), pp. 59–70.

[25] Walter E. Garrey. *The Nature of Fibrillary Contraction of the Heart. - Its Relation to Tissue Mass and Form*. American Physiological Society, 1914, p. 18.

[26] Gordon K. Moe, Werner C. Rheinboldt, and J. A. Abildskov. "A computer model of atrial fibrillation". In: *Am Heart J* 67.2 (1964), pp. 200–220.

[27] M. A. Allessie et al. "Experimental evaluation of Moe's multiple wavelet hypothesis of atrial fibrillation". In: *Cardiac Electrophysiology and Arrhythmias*. Ed. by D. P. Zipes and J. Jalife. Grune & Stratton, 1985, pp. 265–276.

[28] K. T. Konings et al. "High-density mapping of electrically induced atrial fibrillation in humans". In: *Circulation* 89.4 (1994), pp. 1665–80.

[29] R.J Schilling et al. "Endocardial mapping of atrial fibrillation in the human right atrium using a non-contact catheter". In: *Eur Heart J* 21.7 (2000), pp. 550–564.

[30] Koichiro Kumagai, Celeen Khrestian, and Albert L. Waldo. "Simultaneous Multisite Mapping Studies During Induced Atrial Fibrillation in the Sterile Pericarditis Model". In: *Insights Into the Mechanism of its Maintenance* 95.2 (1997), pp. 511–521.

[31] D. Scherf, F. J. Romano, and R. Terranova. "Experimental studies on auricular flutter and auricular fibrillation". In: *Am Heart J* 36.2 (1948), pp. 241–251.

[32] Michel Haïssaguerre et al. "Spontaneous Initiation of Atrial Fibrillation by Ectopic Beats Originating in the Pulmonary Veins". In: *New England Journal of Medicine* 339.10 (1998), pp. 659–666.

[33] Shih-Ann Chen et al. "Radiofrequency catheter ablation of atrial fibrillation initiated by spontaneous ectopic beats". In: *Current Cardiology Reports* 2.4 (2000), pp. 322–328.

[34] C. F. Tsai et al. "Initiation of atrial fibrillation by ectopic beats originating from the superior vena cava: electrophysiological characteristics and results of radiofrequency ablation". In: *Circulation* 102.1 (2000), pp. 67–74.

[35] Sanjiv M. Narayan et al. “Treatment of Atrial Fibrillation by the Ablation of Localized Sources: CONFIRM (Conventional Ablation for Atrial Fibrillation With or Without Focal Impulse and Rotor Modulation) Trial”. In: *J Am Coll Cardiol* 60.7 (2012), pp. 628–636.

[36] Sanjiv M. Narayan, David E. Krummen, and Wouter-Jan Rappel. “Clinical Mapping Approach To Diagnose Electrical Rotors and Focal Impulse Sources for Human Atrial Fibrillation”. In: *J Cardiovasc Electrophysiol* 23.5 (2012), pp. 447–454.

[37] Jay Chen et al. “Dynamics of wavelets and their role in atrial fibrillation in the isolated sheep heart”. In: *Cardiovascular Research* 48.2 (2000), pp. 220–232.

[38] Prashanthan Sanders et al. “Spectral Analysis Identifies Sites of High-Frequency Activity Maintaining Atrial Fibrillation in Humans”. In: *Circulation* 112.6 (2005), pp. 789–797.

[39] H. Calkins et al. “Treatment of atrial fibrillation with antiarrhythmic drugs or radiofrequency ablation: two systematic literature reviews and meta-analyses”. In: *Circ Arrhythm Electrophysiol* 2.4 (2009), pp. 349–61.

[40] A. L. Waldo. “Management of atrial fibrillation: the need for AFFIRMative action. AFFIRM investigators. Atrial Fibrillation Follow-up Investigation of Rhythm Management”. In: *Am J Cardiol* 84.6 (1999), pp. 698–700.

[41] H.P. Rang and M.M. Dale. *Pharmacology*. Churchill Livingstone, 2003.

[42] S. D. Corley et al. “Relationships between sinus rhythm, treatment, and survival in the Atrial Fibrillation Follow-Up Investigation of Rhythm Management (AFFIRM) Study”. In: *Circulation* 109.12 (2004), pp. 1509–13.

[43] K. M. Flegel, M. J. Shipley, and G. Rose. “Risk of stroke in non-rheumatic atrial fibrillation”. In: *Lancet* 1.8532 (1987), pp. 526–9.

[44] J. L. Cox et al. “The surgical treatment of atrial fibrillation. II. Intraoperative electrophysiologic mapping and description of the electrophysiologic basis of atrial flutter and atrial fibrillation”. In: *J Thorac Cardiovasc Surg* 101.3 (1991), pp. 406–26.

[45] J. L. Cox, R. B. Schuessler, and J. P. Boineau. “The surgical treatment of atrial fibrillation. I. Summary of the current concepts of the mechanisms of atrial flutter and atrial fibrillation”. In: *J Thorac Cardiovasc Surg* 101.3 (1991), pp. 402–5.

[46] J. L. Cox et al. “Surgery for atrial fibrillation”. In: *Semin Thorac Cardiovasc Surg* 1.1 (1989), pp. 67–73.

[47] J. L. Cox et al. “The surgical treatment of atrial fibrillation. III. Development of a definitive surgical procedure”. In: *J Thorac Cardiovasc Surg* 101.4 (1991), pp. 569–83.

[48] J. L. Cox et al. “Current status of the Maze procedure for the treatment of atrial fibrillation”. In: *Semin Thorac Cardiovasc Surg* 12.1 (2000), pp. 15–9.

[49] Sunil M. Prasad et al. “The Cox maze III procedure for atrial fibrillation: long-term efficacy in patients undergoing lone versus concomitant procedures”. In: *J Thorac Cardiovasc Surg* 126.6 (2003), pp. 1822–1827.

[50] Akira T. Kawaguchi et al. “Risks and Benefits of Combined Maze Procedure for Atrial Fibrillation Associated With Organic Heart Disease1”. In: *J Am Coll Cardiol* 28.4 (1996), pp. 985–990.

[51] J.P. Joseph and K. Rajappan. “Radiofrequency ablation of cardiac arrhythmias: past, present and future”. In: *QJM* 105.4 (2012), pp. 303–314.

[52] W. M. Jackman et al. “Catheter ablation of accessory atrioventricular pathways (Wolff-Parkinson-White syndrome) by radiofrequency current”. In: *N Engl J Med* 324.23 (1991), pp. 1605–11.

[53] T. Deneke et al. “Histopathology of intraoperatively induced linear radiofrequency ablation lesions in patients with chronic atrial fibrillation”. In: *Eur Heart J* 26.17 (2005), pp. 1797–803.

[54] Marcin Kowalski et al. “Histopathologic Characterization of Chronic Radiofrequency Ablation Lesions for Pulmonary Vein Isolation”. In: *J Am Coll Cardiol* 59.10 (2012), pp. 930–938.

[55] Troy J. Badger et al. “Evaluation of Left Atrial Lesions after Initial and Repeat Atrial Fibrillation Ablation: Lessons learned from Delayed-Enhancement MRI in Repeat Ablation Procedures”. In: *Circ Arrhythm Electrophysiol* 3.3 (2010), pp. 249–259.

[56] M. Haissaguerre et al. “Catheter ablation of long-lasting persistent atrial fibrillation: critical structures for termination”. In: *J Cardiovasc Electrophysiol* 16.11 (2005), pp. 1125–37.

[57] F. Gaita et al. “Long-term clinical results of 2 different ablation strategies in patients with paroxysmal and persistent atrial fibrillation”. In: *Circ Arrhythm Electrophysiol* 1.4 (2008), pp. 269–75.

[58] Hakan Oral et al. “Pulmonary Vein Isolation for Paroxysmal and Persistent Atrial Fibrillation”. In: *Circulation* 105.9 (2002), pp. 1077–1081.

[59] R. R. Tilz et al. “Catheter ablation of long-standing persistent atrial fibrillation: 5-year outcomes of the Hamburg Sequential Ablation Strategy”. In: *J Am Coll Cardiol* 60.19 (2012), pp. 1921–9.

[60] D. Schreiber et al. “Five-year follow-up after catheter ablation of persistent atrial fibrillation using the stepwise approach and prognostic factors for success”. In: *Circ Arrhythm Electrophysiol* 8.2 (2015), pp. 308–17.

[61] M. Hocini et al. “Techniques, evaluation, and consequences of linear block at the left atrial roof in paroxysmal atrial fibrillation: a prospective randomized study”. In: *Circulation* 112.24 (2005), pp. 3688–96.

[62] Karen T.S. Konings et al. “Configuration of Unipolar Atrial Electrograms During Electrically Induced Atrial Fibrillation in Humans”. In: *Circulation* 95.5 (1997), pp. 1231–1241.

[63] Koonlawee Nademanee et al. “A new approach for catheter ablation of atrial fibrillation: mapping of the electrophysiologic substrate”. In: *J Am Coll Cardiol* 43.11 (2004), pp. 2044–2053.

[64] Sanjay Dixit et al. “Randomized Ablation Strategies for the Treatment of Persistent Atrial Fibrillation: RASTA Study”. In: *Circulation: Arrhythmia and Electrophysiology* 5.2 (2012), pp. 287–294.

[65] I. Deisenhofer et al. “Does electrogram guided substrate ablation add to the success of pulmonary vein isolation in patients with paroxysmal atrial fibrillation? A prospective, randomized study”. In: *J Cardiovasc Electrophysiol* 20.5 (2009), pp. 514–21.

[66] C. S. Elayi et al. “Ablation for longstanding permanent atrial fibrillation: results from a randomized study comparing three different strategies”. In: *Heart Rhythm* 5.12 (2008), pp. 1658–64.

[67] J. M. Nuhrich et al. “Impact of biatrial defragmentation in patients with paroxysmal atrial fibrillation: results from a randomized prospective study”. In: *Heart Rhythm* 11.9 (2014), pp. 1536–42.

[68] M. Chen et al. “Randomized comparison between pulmonary vein antral isolation versus complex fractionated electrogram ablation for paroxysmal atrial fibrillation”. In: *J Cardiovasc Electrophysiol* 22.9 (2011), pp. 973–81.

[69] H. Oral et al. “A randomized assessment of the incremental role of ablation of complex fractionated atrial electrograms after antral pulmonary vein isolation for long-lasting persistent atrial fibrillation”. In: *J Am Coll Cardiol* 53.9 (2009), pp. 782–9.

[70] A. Verma et al. “A prospective, multicenter evaluation of ablating complex fractionated electrograms (CFEs) during atrial fibrillation (AF) identified by an automated mapping algorithm: acute effects on AF and efficacy as an adjuvant strategy”. In: *Heart Rhythm* 5.2 (2008), pp. 198–205.

[71] Luigi Di Biase et al. “Atrial Fibrillation Ablation Strategies for Paroxysmal Patients: Randomized Comparison Between Different Techniques”. In: *Circulation: Arrhythmia and Electrophysiology* 2.2 (2009), pp. 113–119.

[72] A. Verma et al. “Approaches to catheter ablation for persistent atrial fibrillation”. In: *N Engl J Med* 372.19 (2015), pp. 1812–22.

[73] Atul Verma et al. “Substrate and Trigger Ablation for Reduction of Atrial Fibrillation (STAR AF): a randomized, multicentre, international trial”. In: *Eur Heart J* 31.11 (2010), pp. 1344–1356.

[74] Omer Berenfeld et al. “Spatially Distributed Dominant Excitation Frequencies Reveal Hidden Organization in Atrial Fibrillation in the Langendorff-Perfused Sheep Heart”. In: *J Cardiovasc Electrophysiol* 11.8 (2000), pp. 869–879.

[75] Felipe Atienza et al. “Real-time Dominant Frequency Mapping and Ablation of Dominant-Frequency Sites in Atrial Fibrillation with Left-to-Right Frequency Gradients Predicts Long-Term Maintenance of Sinus Rhythm”. In: *Heart Rhythm* 6.1 (2009), pp. 33–40.

[76] P. Sommer et al. “Successful Repeat Catheter Ablation of Recurrent Longstanding Persistent Atrial Fibrillation With Rotor Elimination as the Procedural Endpoint: A Case Series”. In: *J Cardiovasc Electrophysiol* 27.3 (2016), pp. 274–80.

[77] Eric Buch et al. “Long-term clinical outcomes of focal impulse and rotor modulation for treatment of atrial fibrillation: A multicenter experience”. In: *Heart Rhythm* 13.3 (2016), pp. 636–641.

[78] A. L. Hodgkin and A. F. Huxley. “A quantitative description of membrane current and its application to conduction and excitation in nerve”. In: *The Journal of Physiology* 117.4 (1952), pp. 500–544.

[79] Mary M. Maleckar et al. “Mathematical simulations of ligand-gated and cell-type specific effects on the action potential of human atrium”. In: *Progress in Biophysics and Molecular Biology* 98.2-3 (2008), pp. 161–170.

[80] Eleonora Grandi et al. “Human Atrial Action Potential and Ca2+ Model: Sinus Rhythm and Chronic Atrial Fibrillation”. In: *Circ Res* 109.9 (2011), pp. 1055–1066.

[81] Jussi T. Koivumäki, Topi Korhonen, and Pasi Tavi. “Impact of Sarcoplasmic Reticulum Calcium Release on Calcium Dynamics and Action Potential Morphology in Human Atrial Myocytes: A Computational Study”. In: *PLoS Comput Biol* 7.1 (2011), e1001067.

[82] A. Nygren et al. “Mathematical model of an adult human atrial cell: the role of K+ currents in repolarization”. In: *Circ Res* 82.1 (1998), pp. 63–81.

[83] M. Courtemanche, R. J. Ramirez, and S. Nattel. “Ionic targets for drug therapy and atrial fibrillation-induced electrical remodeling: insights from a mathematical model”. In: *Cardiovasc Res* 42.2 (1999), pp. 477–89.

[84] Peter S. Spector et al. “Emergence of Complex Behavior: An Interactive Model of Cardiac Excitation Provides a Powerful Tool for Understanding Electrical Propagation”. In: *Circulation: Arrhythmia and Electrophysiology* (2011).

Chapter 3

Mapping Multi-Wavelet Reentry Without Isochrones: An Electrogram Guided Approach to Define Substrate Distribution

Bryce E Benson, BS^{1}, Richard Carrick, $BS^{1,2}$, Nicole Habel, MD^{2}, Oliver Bates, $BEng^{3}$, Jason HT Bates, PhD, $DSc^{1,2}$, Philipp Bielau[2] and Peter Spector, MD^{2}

[1]University of Vermont College of Mathematics and Engineering, Burlington, VT;

[2]University of Vermont College of Medicine, Burlington, VT;

[3]Boston University College of Engineering, Boston, MA

3.1 Abstract

Background: A key mechanism responsible for atrial fibrillation is multi-wavelet reentry (MWR). We have previously demonstrated that ablation in regions of increased circuit-density reduces the duration of, and decreases the inducibility of MWR. In this study we demonstrate a method for identifying local circuit-density using electrogram frequency and validated its effectiveness for map-guided ablation in a computer model of MWR.

Methods and Results: We simulated MWR in tissues with variation of action poten-

tial duration and intercellular resistance. Electrograms were calculated using various electrode sizes and configurations. We measured and compared the number of circuits to the tissue activation frequency and electrogram frequency using three recording configurations (unipolar, contact bipolar, orthogonal closed unipolar (OCU)) and two frequency measurements (dominant frequency, centroid frequency). We then used the highest resolution electrogram frequency map (OCU centroid frequency) to guide the placement of lesions to high frequency regions. Map guided ablation was compared with no ablation and random/blind ablation lesions of equal length. Electrogram frequency correlated with tissue frequency and circuit-density as a function of electrode spatial resolution. Map-guided ablation resulted in a significant reduction in MWR duration (142±174s vs. 41±63s).

Conclusion: Electrogram frequency correlates with circuit-density in MWR provided electrodes have high spatial resolution. Map-guided ablation is superior to no ablation and to blind/random ablation.

3.2 Introduction

Atrial fibrillation (AF) affects over 5 million people in the United States alone and results in a cost to the US healthcare system estimated to be between 6 and 26 billion dollars per year[1]. Despite its impact treatments remain less than adequate, particularly for persistent AF. Anti-arrhythmics work poorly, maintaining sinus rhythm in only approximately 45% of patients. Ablation is only marginally better, effectively treating only approximately 50% of patients with persistent AF[2]. Ablation is much more effective when one can guide lesion placement by defining the arrhythmia circuit

through mapping; for example 92% in AFL[3]. Unfortunately, due to the dynamic and complex nature of activation during fibrillation, it is very difficult to define the circuitry responsible for arrhythmia perpetuation in individual patients with the use of activation mapping[4, 5].

We have previously demonstrated that ablation lesions which target regions of high circuit-density maximize the effectiveness of ablation for multi-wavelet reentry (MWR)[6, 7]. In this paper, we describe an algorithm for identifying circuit-core-density and distribution during multi-wavelet reentry based upon high resolution electrogram frequency mapping and validate its efficacy through a map guided ablation trial. High resolution frequency mapping does not require activation mapping; identification of circuits without the use of isochronal maps obviates the need to overcome the engineering hurdles inherent in creating full activation maps of MWR (e.g. large numbers of closely spaced and high resolution electrodes).

3.2.1 Theoretical Foundation

We hypothesized that during MWR 1) circuit distribution is dependent upon the heart's electrophysiologic properties, 2) those areas with the shortest wavelength would have the highest probability of containing a circuit-core and 3) would (on average) be excited more frequently than other heart regions. Thus if one could accurately identify local tissue excitation frequency this would indirectly identify circuit-density. Unfortunately, in the clinical setting one cannot directly measure tissue activation (or its frequency); rather we are dependent upon electrogram recordings to identify cardiac electrical events. Electrogram frequency reflects the frequency of electrical activity within the recording region of the electrode(s); therefore, electrogram fre-

quency may not accurately reflect the activation frequency of any individual cell but rather the ensemble frequency of a group of cells. If there is electrical dyssynchrony within the group of cells recorded, then the electrogram frequency may not be the same as any individual cell in the group. Therefore, electrogram frequency accurately reflects tissue frequency only if the spatial resolution of the recording electrode(s) encompasses a region of tissue that is synchronously activated.

3.3 Methods

3.3.1 Model and Tissue Setup

In order to assess the accuracy of electrogram mapping the true map must be known precisely. In biological systems the details of electrical activity are very difficult to discern. Accordingly, we used a computational model of electrical excitation in which precisely controlled and fully known electrical activity can be generated. We used a physics-based cellular automaton model previously described[8]. Our model consists of a two dimensional array of electrically excitable cells (each representing a large group of myocytes) connected via resistive pathways. Each cell generates an action potential when it receives sufficient current from neighboring cells and subsequently undergoes a period of refractoriness during which it cannot be re-excited. The exact characteristics of each cell's action potential are determined by 1) its programmed baseline parameters (including restitution) and 2) electrotonic current shifts. Intercellular resistance is user defined.

We created 9 test tissues with varied physiologic properties. Each tissue consists

of a 2-dimensional sheet of cells - "tissue" (80x80mm^2) (Figure 3.1a). Each cell's action potential duration (APD) is randomly chosen from a programmed mean and standard deviation. To produce tissues with regional circuit-density heterogeneity we created patches of cells with shorter average APD and higher intercellular resistance than the remainder of the tissue - "patch". Varying the number of patches and tissue parameters produced variations of circuit-density gradients and distributions.

The tissues each contained 1-3 short wave-length patches. All "patches" had APDs of 80±5ms and intercellular resistance of 13ohms. "Tissues" were comprised of APDs of 110±10ms, 120±10ms or 130±10ms (intercellular resistance was 9ohms in each case).

3.3.2 Electrogram Recordings

Electrograms were calculated using both unipolar and bipolar electrode configurations from 100 recording sites distributed over each tissue. Electrodes were cylindrical; each created using a finite element mesh (element-area 0.75mm^2, element-number varied with electrode size); electrograms were calculated as described previously[9]. All recordings were made from a 10x10 (evenly spaced) array of recording sites, 1mm above the tissue. For unipolar recordings (UNI), a single electrode was placed at each recording site. Contact bipolar electrograms (CBP) were recorded by placing a pair of electrodes (2mm inter-electrode distance) centered over each recording site. A second array of electrodes (2mm) above the unipolar array allowed creation of bipolar pairs arranged orthogonal to the tissue surface ("orthogonal close unipolar" [10] (OCU)). For the UNI and OCU configurations, electrograms were generated with both small (1mm diameter/height) and large (3mm diameter/height) electrodes (only the small

electrodes were used for the CBP configuration). Figure 3.1b shows an example of electrograms generated from each of the recording configurations.

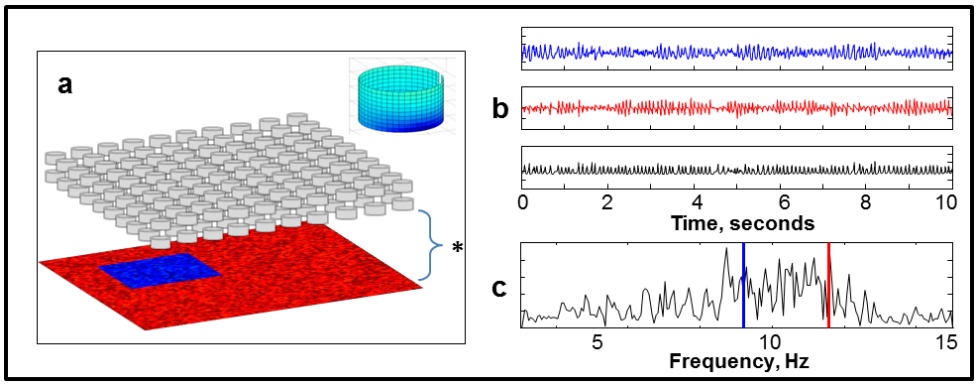

Figure 3.1: Experimental setup and electrogram analysis. a) High-resolution frequency mapping setup. Red and blue rectangles represent 2 dimensional sheet of tissue, action potential duration varies through tissue (red "cells" have longer APD, blue cells have shorter APD). Gray cylinders represent electrode array (height of electrodes [*] is exaggerated in figure). Inset: a finite element electrode mesh. b) Electrograms (UNI [blue], CBP [red], and OCU [black]). c) Power spectrum generated from a unipolar electrogram demonstrating the difference between DF (red line) and CF (blue line).

3.3.3 Circuit-Density

We required an accurate (and computationally tractable) algorithm for identification of circuit-density. One standard approach to circuit identification is through transformation of activation-maps into phase-maps and the subsequent identification of phase-singularities[11] (PS). This has some limitations, including high computational burden, false positive identification of cores and failure to identify circuit-cores that are not phase singularities (i.e. larger cores). Therefore, we developed an algorithm that 1) identified wave ends and 2) tracked those wave ends through space-time

until they returned to a previously occupied location forming a closed circuit (Figure 3.2). The area encompassed by this closed loop is defined as being a single instance of a circuit-core. A circuit-density (Cd) map was then constructed as the sum of all circuits identified over the recording period.

We compared the accuracy of closed-loop and PS-mapping against using direct visualization as our gold standard (activation was tracked every millisecond for 500ms of MWR). We calculated a 2D correlation with both the closed-loop and PS maps. Correlation was calculated as:

$$r = \frac{\sum_m \sum_n \left[A_{mn} - \bar{A}\right] \left[B_{mn} - \bar{B}\right]}{\sqrt{\sum_m \sum_n \left[A_{mn} - \bar{A}\right]^2 \left[B_{mn} - \bar{B}\right]^2}} \tag{3.1}$$

where A and B are the tissue frequency and circuit-density matrices, respectively. The sensitivity of each was calculated as:

$$Sensitivity = \frac{TP}{TP - FN} \tag{3.2}$$

where TP (true positive) is the number of circuits correctly identified and FN (false negative) is the number of circuits not identified by the algorithm. Computation time was measured.

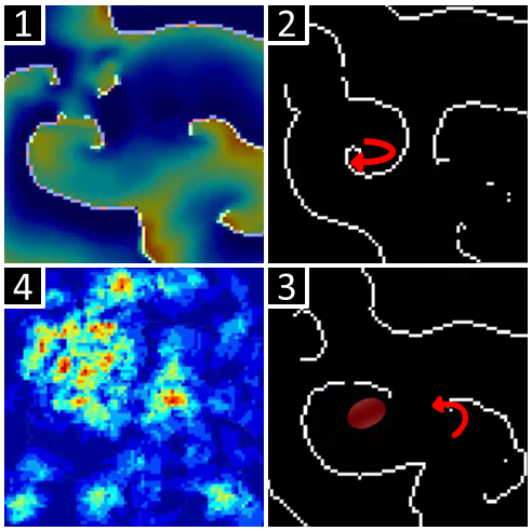

Figure 3.2: Circuit density mapping. 1) Leading edge of excitation is identified in voltage map. 2) Wave-end paths are tracked. 3) Closed loops and their enclosed areas are identified. 4) Circuit-density map = sum of all closed loops.

3.3.4 Tissue and Electrogram Frequencies

Multi-wavelet reentry was induced with burst pacing (cycle-length 50ms x 2s). Induction was attempted sequentially from 16 locations (4x4 evenly distributed pacing sites). Cell voltages and electrogram potentials were recorded for 10s of MWR. Time to termination was measured. Tissue activation frequency (TF) (determined directly from membrane voltages) was calculated for each cell as the inverse of the average cycle-length during 10s of MWR. Circuit-density and tissue frequency maps were compared using a 2D correlation (equation 1).

Electrograms frequencies calculated with a fast Fourier transform (FFT). Frequency was characterized as: 1) dominant frequency (DF) (largest peak in the power

spectrum) and 2) centroid frequency (CF) (geometric center /arithmetic mean frequency; calculated as:

$$Centroid = \frac{\int_3^{15} F * Y(F) dF}{\int_3^{15} Y(F) dF} \tag{3.3}$$

where F is the frequency and Y is the amplitude in the power spectrum). Figure 3.1c shows an example of the DF and CF.

Electrogram frequencies (of UNI, CBP and OCU recordings) were compared to TF and Cd of the cells immediately beneath the footprint of each electrode. Correlation coefficients were calculated as:

$$r = \frac{\sum_{i=1}^{n} \left[X_i - \bar{X}\right] \left[Y_i - \bar{Y}\right]}{\sqrt{\sum_{i=1}^{n} \left[X_i - \bar{X}\right]^2} \sqrt{\left[Y_i - \bar{Y}\right]^2}} \tag{3.4}$$

where X and Y represent the electrogram frequency and tissue activation frequency. Maps were created by assigning the electrogram frequency (DF or CF) to each recording site and performing a least squares interpolation (Figure 3.3).

3.3.5 Ablation Protocol

We compared map-guided with blind/random ablation. In each of the nine tissues, MWR was induced and allowed to perpetuate up to a maximum of 10 minutes. We measured the time to termination with map-guided and blind/random ablation. For map-guidance we used the highest-resolution frequency maps (OCU, small electrodes, centroid frequency). Linear lesions were distributed such that 1) lesions were always connected to one of the tissue's outer boundaries and 2) lines covered the areas with highest circuit-density. Blinded/random lesions were applied to each tissue

by randomly selecting target sites in the tissue and placing a lesion from an existing boundary to the target (Figure 3.6). The length of lesions (38mm, 59mm, and 86mm for 1, 2 and 3 patches respectively) used for both the blind/random and guided approaches remained equal for all tissues.

3.3.6 Statistical Analysis

We compared circuit-density and frequency inside and outside the patch(es). Data are presented as mean ± standard deviation. Paired student's t-test was used to compare differences. Statistically significant differences were defined as $p<0.01$.

3.4 Results

3.4.1 Quantifying Circuit-Density

We compared the circuit-density and phase-singularity mapping algorithms against visual inspection of circuits. The Cd algorithm had a sensitivity of 0.79 and a correlation coefficient of 0.76. The PS map had a sensitivity of 0.53 and a correlation coefficient of 0.46. Computation time (for 500ms of MWR) was 14.9s (Cd algorithm) vs. 98.3s (PS algorithm).

Table 3.1: Tissue frequency, circuit-density and electrogram frequency (average±SD) inside and outside the patch region (low, medium and high circuit-gradient).

		TF	Cd	UNI CF	UNI DF	CBP CF	CBP DF	OCU CF	OCU DF
Inside	Low	11.82± 0.1	50.10± 13.6	9.24± 0.1	10.36± 0.2	10.32± 0.1	10.93± 0.2	10.11± 0.1	10.90± 0.2
	Med	11.38± 0.2	37.80± 13.4	9.03± 0.1	9.73± 0.2	10.09± 0.1	10.31± 0.3	9.92± 0.1	10.33± 0.3
	High	11.08± 0.2	27.54± 10.4	8.86± 0.1	9.12± 0.2	9.92± 0.1	9.77± 0.3	9.78± 0.1	9.88± 0.3
Outside	Low	10.91± 0.2	20.15± 10.6	9.14± 0.1	10.47± 0.1	10.10± 0.1	10.79± 0.2	9.80± 0.1	10.71± 0.1
	Med	10.10± 0.2	14.83± 8.9	8.85± 0.1	9.69± 0.1	9.79± 0.1	10.01± 0.2	9.48± 0.1	9.90± 0.2
	High	9.45± 0.3	11.31± 7.8	8.65± 0.1	9.05± 0.1	9.57± 0.2	9.38± 0.3	9.25± 0.1	9.26± 0.2

3.4.2 Tissue Frequency vs. Circuit Density

For illustrative purposes figure 3.3 shows examples of patch location (cell property distribution), circuit-density and tissue frequencies in tissues with patches of random dimension. In the test-tissues circuit-density (#circuits/mm^2 /10s) was higher inside than outside the patches (38±16 vs. 15±10, inside vs. outside respectively; $p<0.001$). Tissue frequency was higher inside than outside the short wave-length

patches (11.4±0.4 vs. 10.2±0.6, inside vs. outside respectively; $p<0.001$). There was a strong correlation between TF and Cd ($r^2=0.59$ all tissues combined). Figure 3.4 shows the correlation coefficient and sensitivity for each tissue. Correlation diminished as the number of high circuit-density patches increased and as the density gradient decreased.

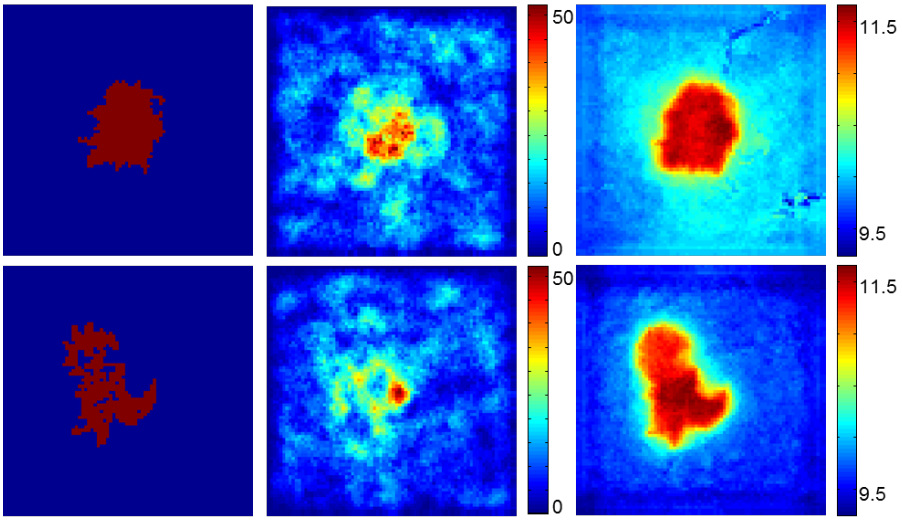

Figure 3.3: Relationship between tissue properties (left), circuit-density (middle) and tissue activation frequency (right). Maps were generated from 10s of MWR.

3.4.3 Electrogram Frequency vs. Tissue Frequency

Table 3.2 shows the correlation coefficients for each electrode configuration. Frequency of unipolar electrograms were the least accurate compared with tissue frequency (DF: $r^2=0.08$, CF: $r^2=0.35$). CBP were more accurate (DF: $r^2=0.20$, CF:

r^2=0.46). OCU most accurately reflected TF (DF: r^2=0.57, CF: r^2=0.93). When all recording configurations were combined centroid frequency was superior to dominant frequency (CF: r^2=0.58, DF: r^2=0.28).

Table 3.2: Correlation between electrogram frequency, circuit-density and tissue activation frequency.

Patches			1			2			3		
Gradient			Low	Med	High	Low	Med	High	Low	Med	High
TF	DF	UNI	0.10	0.01	0.19	0.07	0.17	0.05	0.07	0.00	0.03
		CBP	0.14	0.29	0.53	0.13	0.19	0.15	0.03	0.17	0.17
		OCU	0.15	0.46	0.76	0.62	0.70	0.69	0.39	0.67	0.68
	CF	UNI	0.32	0.52	0.66	0.17	0.34	0.41	0.07	0.33	0.32
		CBP	0.48	0.56	0.68	0.31	0.48	0.50	0.27	0.40	0.47
		OCU	0.90	0.94	0.96	0.88	0.93	0.93	0.95	0.95	0.92
Cd	DF	UNI	0.14	0.03	0.11	0.08	0.10	0.07	0.03	0.02	0.05
		CBP	0.10	0.40	0.55	0.08	0.28	0.43	0.07	0.28	0.33
		OCU	0.06	0.51	0.55	0.47	0.41	0.27	0.24	0.41	0.25
	CF	UNI	0.30	0.40	0.50	0.15	0.32	0.39	0.13	0.22	0.30
		CBP	0.51	0.51	0.58	0.26	0.47	0.44	0.35	0.39	0.45
		OCU	0.72	0.70	0.73	0.56	0.60	0.48	0.60	0.49	0.44

3.4.4 Electrogram Frequency vs. Circuit Density

Similar to the trends seen with electrogram frequency vs. tissue frequency, OCU electrograms more accurately reflected the Cd than UNI or CBP electrograms (table 3.2). Again, CF was superior to DF.

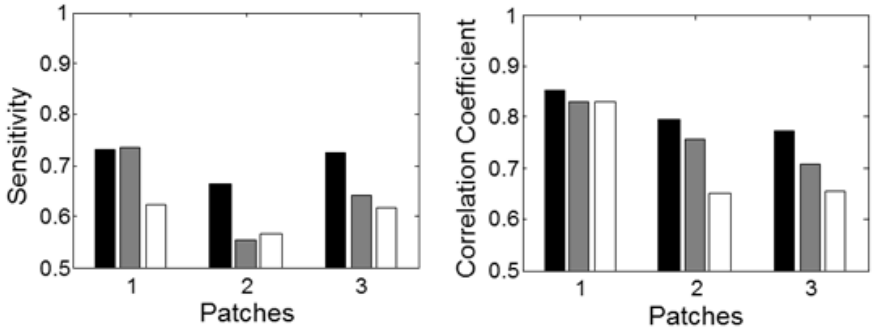

Figure 3.4: Correlation coefficients and sensitivity between circuit-density and tissue activation frequency. Black bars, gray bars and white bars indicate tissues with low, medium and high circuit-density gradient, respectively.

3.4.5 Effect of Electrode Size on Map Accuracy

For both UNI and OCU the correlation between electrogram centroid frequency and circuit-density was higher with smaller electrodes. Correlation decreased with tissue spatial complexity/gradient in Cd (low-gradient $\triangle$r=0.15, medium-gradient $\triangle$r=0.07, high-gradient $\triangle$r=0.02).

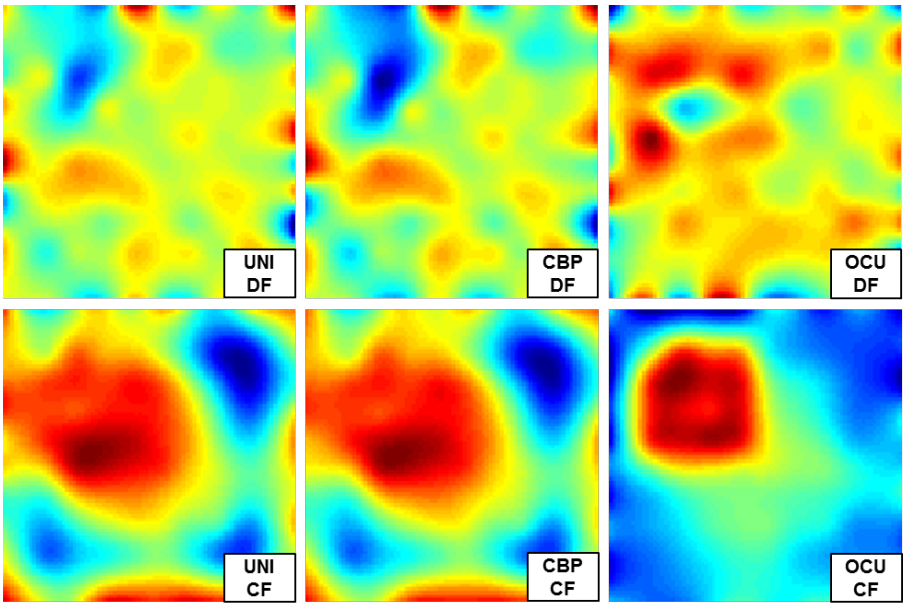

Figure 3.5: Impact of spatial resolution and frequency metric (DF vs. CF) on electrogram frequency maps. The high circuit-density patch was located in the upper left hand corner of the tissue, best seen on the "OCU Centroid" map.

3.4.6 Map Guided Ablation

We compared the impact of map-guided vs. random/blind ablation (and no ablation) on time to termination of MWR. Map-guided ablation resulted in reduction of MWR duration compared with no ablation (142±174s vs. 171±193s vs. 41±63s, no ablation, blind/random ablation, map-guided ablation respectively; p=NS no ablation vs. blind/random ablation, $p<0.001$ no ablation vs. map-guided ablation).

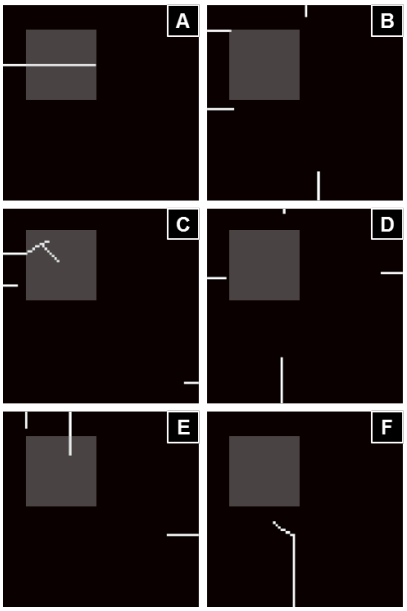

Figure 3.6: Example of ablation lesions for (A) guided and (B-F) several random/blinded ablation lesions. Note that random/blind lesions sometimes overlap the high circuit-density patches (C and E).

3.5 Discussion

3.5.1 Discriminating active drivers from passive followers in multi-wavelet reentry

Defining the substrate responsible for perpetuation of MWR and identifying its distribution is critical for planning ablation strategies that reduce the hearts ability to maintain fibrillation. Using computational modeling we were able to observe tissue excitation in its entirety (e.g. the voltage of every cell for every millisecond during

MWR). Interestingly even direct observation of MWR does not reveal which tissue regions are actively perpetuating the rhythm and which are being passively driven by the rhythm.

We developed a novel method for identifying the circuits that drive MWR. Our method, closed loop mapping, is based upon the necessity for closed circuits in order to maintain continuous activation on a finite surface. Activation paths vary and are dynamically formed by shifting excitability, refractoriness and structurally and/or functionally defined source-sink balance[12]. Circuits can be defined by the full path of activation or by the boundaries of that activation. This is analogous to identifying a road by the extent of the pavement vs. the location of the inner and outer guard rails. In the context of reentrant circuits, the tissue edge is the outer boundary and the circuit-core is the inner boundary. Successful ablation requires complete circuit transection[6] (outer-inner boundary); we know where the tissue edge is therefore the goal of mapping is identification of the inner boundary, i.e. the circuit-core.

We tracked wave ends (the outermost tip of each wave-front) as they traversed the tissue; we defined a circuit-core as the area circumscribed by the loop formed when an internal wave-end (those not connected to the tissue edge) returned to a location it had previously occupied (video). The number of times a given region of tissue was included in a circuit-core was then defined as that region's circuit-core density. This method outperformed PS tracking (greater sensitivity and specificity with lower computational burden).

3.5.2 Circuit-Density vs. Tissue Frequency

One cannot directly observe tissue activation in the clinical setting and hence closed loop tracking cannot be employed in patients. We therefore sought to develop an electrogram guided metric that correlates with circuit-density. We hypothesized that 1) local tissue activation frequency (on average) correlates with circuit-density and 2) electrogram frequency, provided it is recorded by electrodes of adequate spatial resolution, correlates with local tissue frequency. Due to the simultaneous presence of multiple wave-fronts and shifting conduction block during MWR not all cells are activated at the same rate. We reasoned that those cells responsible for driving MWR would activate more frequently, while passively driven cells would at times be activated less frequently due to following the reentrant drivers with less than 1:1 continuity. While it is possible that some cells can be passively driven by 2 separate reentrant circuits and actually be excited more frequently than any individual driver; ultimately, because local tissue properties influence wavelength and hence maximal excitation rates, on average driver regions are activated more rapidly than passive follower regions even if there are times when followers are transiently activated more frequently. Our data indicated that tissue activation frequency correlates with circuit-density over a wide range of conditions.

3.5.3 Tissue vs. Electrogram Frequency

We have previously demonstrated that electrogram frequency does not accurately reflect tissue frequency if the spatial resolution of the electrodes results in simultaneous recording of multiple dissociated muscle fibers[5]. Under these circumstances

one measures the frequency of some combination of dissociated cells and hence the electrogram frequency is not the same as the activation frequency of any individual myocyte. If the electrode's spatial resolution is sufficient to record only synchronously activated cells its electrogram frequency does accurately reflect local tissue frequency. We demonstrated that the accuracy of electrogram frequency for identifying local tissue frequency (and local circuit-density) improves with improving spatial resolution (e.g. orthogonal close unipolar > contact bipolar > unipolar).

3.5.4 Centroid vs. Dominant Frequency

Due to the variability in local activation during MWR both tissue frequency and electrogram frequency, vary over time; fast Fourier transformation reveals a wide spectrum of frequencies. We found that the DF could be quite variable and correlated poorly with tissue frequency whereas the centroid of the power spectrum correlated better with tissue frequency. A frequency range of 3 to 15 Hz was put in place during the calculation of centroid frequency in order to reduce high and low frequency noise as well as evaluate the physiologic range of the signal. This range was chosen to be optimized for this simulated series of atrial fibrillation and may need to be altered for higher or lower frequency AF.

3.5.5 Map-Guided Ablation

Ultimately the purpose of identifying the substrate responsible for perpetuating MWR is to direct therapy to modify that substrate; hence the relevant test of a map's adequacy is its ability to guide effective ablation. We have previously demonstrated

that knowledge of circuit-density distribution can improve ablation efficiency[7]. In this study we examined whether an electrogram guided map could improve ablation when compared with blind/random ablation. Electrogram guided ablation increased the probability of MWR termination (measured as reduction in time to termination) compared with both un-ablated tissue and random ablation (using the same total lesion length). In fact as we have previously shown[7], because ablation at sites of low circuit-density actually increases new wave formation (more than they increase wave annihilation) random ablation was worse than no ablation.

3.5.6 Comparison with previous studies

Multi-wavelet reentry vs. focal driver with fibrillatory conduction

Historically strategies for ablation of AF have been formulated based upon assumptions about its mechanisms. The most commonly employed ablation strategies involve targeting of both focal triggers and modification of the atria's ability to support multi-wavelet reentry. The successes of the surgical and catheter maze procedures[13, 14] strongly suggest that the mechanism of AF (at least in responders) is MWR; unless the maze lesion set coincidently transects the site of focal firing it should limit fibrillatory conduction but not eliminate the focal driver. The lack of success of the maze procedures in non-responders may attest to a focal mechanism in these patients. Alternatively, it may simply be that by delivering non-map guided lesions the maze procedure suffers from insufficient guidance (it is undirected) and insufficient magnitude (it is untitrated). It is quite possible that not all patients with AF have the same underlying mechanism. It is also likely, based upon the remodeling that results from sustained tachycardia, that MWR ultimately plays a crucial role in perpetuation

of AF in the majority of cases. It is therefore of great interest to identify a means for mapping the spatial distribution of the substrate responsible for perpetuation of MWR.

Frequency Mapping

Map-guidance for AF ablation has been the subject of intense research. Several other approaches have been suggested in the past. Frequency mapping developed by Jalife[15] and tested clinically by Haissaguerre[16] conferred little advantage over conventional ablation[17]. This may reflect either inadequacy of the spatial resolution of the recording electrodes and/or the variability of using DF rather than centroid frequency. During MWR tissue frequency is dynamic; there is not therefore a single value for tissue frequency but rather a spectrum. Prior studies have used the dominant frequency as a metric for tissue frequency[16]. We found that the DF can vary based upon small changes in the height of large peaks in the power spectrum; the centroid frequency which reflects the mean frequency is less variable and more reliably correlated with tissue activation frequency in our studies.

Complex Fractionated Atrial Electrograms

Complex fractionated atrial electrograms (CFAE) have also been used widely as targets for ablation[18]. Interestingly, fractionation results from inadequate spatial resolution relative to local tissue spatio-temporal variability[5] (STV). Thus CFAE mapping identifies the distribution of STV. Because STV is related largely to tissue electrophysiologic properties STV (CFAE) mapping reflects somewhat the distribution of tissue physiology. There are two theoretical limitations to CFAE mapping; 1) the

distribution is spatial resolution dependent (i.e. electrode size, inter-electrode spacing and recording configuration dependent) and 2) STV while related to, does not directly correspond with activation frequency. A number of studies have demonstrated a lack of correlation between the distributions of CFAE and DF[19].

Focal Impulse and Rotor Modulation (FIRM)

A more recent approach to mapping AF, FIRM mapping[20], employs an extremely different approach for circuit identification. FIRM mapping identifies circuit-cores by creating and interpreting activation maps. This is done with the use of a relatively small number of electrodes (64) with relatively low spatial resolution (1.25mm, 4 or 5mm inter-electrode spacing). Determination of local activation time despite electrogram fractionation under these circumstances requires assumptions about local refractory times and physiologically possible conduction velocities based upon monophasic action potential recordings. There is none-the-less relatively low sample density so this approach requires interpolation for interpretation of activation and hence identification of circuits. Frequency mapping obviates the need to first reconstruct activation maps and then identify circuits thereby obviating the need for high density mapping.

3.5.7 Limitations

The work described in this study was performed entirely in a computational model of electrical propagation. Ultimately biological confirmation is essential. However, in order to directly establish the links from activation through circuit-core distribution to tissue frequency and finally electrogram frequency one must have the ability to

make direct measurements of each of these quantities. Such information is exceedingly difficult to obtain in biologic preparations yet easily accessible in computational modeling. In addition, modeling allows simultaneous recording using electrodes of varying spatial resolution at the same location during the same episodes of MWR. As a result, the variation between electrograms recorded with different electrodes is attributable only to recording resolution and not to changes between episodes of MWR.

3.6 Conclusions

Improved success rates for ablation of atrial fibrillation are likely to require patient-specific map-guided ablation strategies. We have previously demonstrated that one can achieve a greater reduction in the ability of tissue to support MWR when ablation lesion placement is guided by circuit-density[7]. Our data indicate that circuit-density correlates with average tissue frequency and tissue frequency correlates with electrogram frequency (provided sufficient spatial resolution). Frequency analysis using the centroid of the power spectrum more accurately reflects tissue frequency than does the dominant frequency.

Electrogram guided ablation using this method is superior to blind ablation (which can be worse than no ablation). This work represents an important step in the evolution of ablation techniques for AF: it allows for identification of the substrate responsible for perpetuation of multi-wavelet reentry and does so without the need for high density electrode arrays.

Future work will be needed to determine the optimal electrode design for mapping

of circuit-density. This study indicates that the design of such mapping catheters will require the use of electrodes with adequate spatial resolution to generate maps that accurately reflect local tissue activation frequency. Based upon our prior work, "adequate" spatial resolution is not an absolute quantity but rather is relative to the local spatio-temporal frequency of activation[5]. Clinical studies will be required to identify the range of spatio-temporal frequencies in patients during AF.

Bibliography

[1] M. H. Kim et al. "Estimation of total incremental health care costs in patients with atrial fibrillation in the United States". In: *Circ Cardiovasc Qual Outcomes* 4.3 (2011), pp. 313–20.

[2] H. Calkins et al. "Treatment of atrial fibrillation with antiarrhythmic drugs or radiofrequency ablation: two systematic literature reviews and meta-analyses". In: *Circ Arrhythm Electrophysiol* 2.4 (2009), pp. 349–61.

[3] P. Spector et al. "Meta-analysis of ablation of atrial flutter and supraventricular tachycardia". In: *Am J Cardiol* 104.5 (2009), pp. 671–7.

[4] N. Habel et al. "The temporal variability of dominant frequency and complex fractionated atrial electrograms constrains the validity of sequential mapping in human atrial fibrillation". In: *Heart Rhythm* 7.5 (2010), pp. 586–93.

[5] D. D. Correa de Sa et al. "Electrogram fractionation: the relationship between spatiotemporal variation of tissue excitation and electrode spatial resolution". In: *Circ Arrhythm Electrophysiol* 4.6 (2011), pp. 909–16.

[6] P. S. Spector et al. "Ablation of multi-wavelet re-entry: general principles and in silico analyses". In: *Europace* 14 Suppl 5 (2012), pp. v106–v111.

[7] R. T. Carrick et al. "Ablation of multiwavelet re-entry guided by circuit-density and distribution: maximizing the probability of circuit annihilation". In: *Circ Arrhythm Electrophysiol* 6.6 (2013), pp. 1229–35.

[8] Peter S. Spector et al. "Emergence of Complex Behavior: An Interactive Model of Cardiac Excitation Provides a Powerful Tool for Understanding Electrical Propagation". In: *Circulation: Arrhythmia and Electrophysiology* (2011).

[9] J. M. Stinnett-Donnelly et al. "Effects of electrode size and spacing on the resolution of intracardiac electrograms". In: *Coron Artery Dis* 23.2 (2012), pp. 126–32.

[10] N. C. Thompson et al. "Improved spatial resolution and electrogram wave direction independence with the use of an orthogonal electrode configuration". In: *J Clin Monit Comput* 28.2 (2014), pp. 157–63.

[11] R. Zou et al. "Development of a computer algorithm for the detection of phase singularities and initial application to analyze simulations of atrial fibrillation". In: *Chaos* 12.3 (2002), pp. 764–778.

[12] P. Spector. “Principles of cardiac electric propagation and their implications for re-entrant arrhythmias”. In: *Circ Arrhythm Electrophysiol* 6.3 (2013), pp. 655–61.

[13] J. L. Cox et al. “Five-year experience with the maze procedure for atrial fibrillation”. In: *Ann Thorac Surg* 56.4 (1993), pp. 814–823, 814–823.

[14] T. Weimar et al. “The cox-maze procedure for lone atrial fibrillation: a single-center experience over 2 decades”. In: *Circ Arrhythm Electrophysiol* 5.1 (2012), pp. 8–14.

[15] Omer Berenfeld et al. “Spatially Distributed Dominant Excitation Frequencies Reveal Hidden Organization in Atrial Fibrillation in the Langendorff-Perfused Sheep Heart”. In: *J Cardiovasc Electrophysiol* 11.8 (2000), pp. 869–879.

[16] Prashanthan Sanders et al. “Spectral Analysis Identifies Sites of High-Frequency Activity Maintaining Atrial Fibrillation in Humans”. In: *Circulation* 112.6 (2005), pp. 789–797.

[17] A. Verma et al. “Relationship between complex fractionated electrograms (CFE) and dominant frequency (DF) sites and prospective assessment of adding DF-guided ablation to pulmonary vein isolation in persistent atrial fibrillation (AF)”. In: *J Cardiovasc Electrophysiol* 22.12 (2011), pp. 1309–16.

[18] Koonlawee Nademanee et al. “A new approach for catheter ablation of atrial fibrillation: mapping of the electrophysiologic substrate”. In: *J Am Coll Cardiol* 43.11 (2004), pp. 2044–2053.

[19] M. K. Stiles et al. “High-density mapping of atrial fibrillation in humans: relationship between high-frequency activation and electrogram fractionation”. In: *J Cardiovasc Electrophysiol* 19.12 (2008), pp. 1245–53.

[20] Sanjiv M. Narayan, David E. Krummen, and Wouter-Jan Rappel. “Clinical Mapping Approach To Diagnose Electrical Rotors and Focal Impulse Sources for Human Atrial Fibrillation”. In: *J Cardiovasc Electrophysiol* 23.5 (2012), pp. 447–454.

Chapter 4

Mapping Multi-wavelet Reentry: An Electrogram Derived Metric to Identify Tissue Contact

Bryce E Benson, BS^{1}, Richard Carrick, $BS^{1,2}$, Nicole Habel, MD^{2}, Jason HT Bates, PhD, $DSc^{1,2}$, and Peter Spector, MD^{2}

[1]University of Vermont College of Mathematics and Engineering, Burlington, VT;

[2]University of Vermont College of Medicine, Burlington, VT

4.1 Abstract

Background: We have previously demonstrated that identification of circuit core distribution during multi-wavelet reentry can guide effective ablation. Using high spatial resolution electrodes, electrogram frequency correlates with circuit core density. However, here we demonstrate electrogram frequency varies with electrode height. Therefore, we developed and tested a new algorithm to identify catheter tissue contact via comparison of the time derivative of the electrogram potential (dV/dt) between two electrodes oriented orthogonal to the heart surface.

Methods: Using computational studies and confirmed with swine epicardial mapping, we recorded electrograms in sinus rhythm and atrial fibrillation. The first derivative of

each unipolar electrogram was calculated and the maximum dV/dt of the 30 highest peaks was measured. The efficacy of this measure to identify tissue contact was evaluated in both simulated and swine models of AF.

Results: Electrogram frequency decreased as a function of increasing height by a degree that varied with AF frequency (0.4 ± 0.1 Hz (7Hz AF) to 2 ± 0.5 Hz (9Hz AF)). The difference in dV/dt decreased exponentially as a function of increasing distance to the tissue. Mapping of simulated multi-wavelet reentry using electrodes of randomly varied heights produced inaccurate frequency maps (r^2=0.6). Excluding electrodes > 2mm improved accuracy (r^2 =0.96) and delta dV/dt produced results similar to direct height measurements (r^2=0.94).

Conclusions: The accuracy of electrogram frequency mapping is dependent on the electrode distance to the tissue surface. Catheter-tissue contact can be identified with electrogram analysis alone.

4.2 Introduction

Atrial fibrillation (AF) is a common cardiac arrhythmia contributing to a large burden on cardiac health. Despite its complications, it has remained problematic to treat both pharmacologically and interventionally. Traditional catheter ablation (pulmonary vein isolation) has shown modest success in patients with paroxysmal AF, but success rates diminish in progressed forms of the disease. This is largely due to the failure of this method to identify and target the substrate responsible for AF maintenance.

We previously demonstrated that identification of circuit core distribution during

multi-wavelet reentry can guide effective ablation [1]. Furthermore, we found that the tissue frequency distribution could be used as a surrogate for the identification of the circuit density. Provided high electrode spatial resolution, electrogram frequency correlates with both tissue frequency and circuit core distribution and could be used as a guide for targeted ablation [2].

While certain aspects of spatial resolution are controllable such as the size of the recording electrode and the configuration of electrodes within a recording site (unipolar recordings vs. bipolar recordings), the distance between an electrode and the tissue surface is difficult to identify clinically. In this paper, we investigate the change in electrogram morphology as a result of increasing electrode distance to the tissue surface and propose an electrogram derived tool to identify proper electrode-tissue contact and orientation. To further improve the accuracy of electrogram frequency mapping, a method for filtering fractionation from the electrogram signal is proposed.

4.3 Methods

4.3.1 Model of Excitable Media

To assess the robustness of electrogram frequency to changes in spatial resolution and electrode position, we utilized a reproducible model of cardiac electrical propagation described previously [3]. The model consists of a two dimensional grid of excitable "cells" (each representing a group of myocytes) which are electrically connected via resistive pathways in von Neumann neighborhoods (cells sharing edges). Neighboring cells exchange current according to their voltage difference and intercel-

lular resistance, R. When the voltage of a cell exceeds a user defined threshold, an action potential is initiated and the cell cannot be re-excited for the duration of its refractory period (APD). The morphology of an action potential is determined by its pre-programmed intrinsic behavior (upstroke, plateau, and repolarization phase durations) and the extrinsic current exchanges with neighboring cells.

4.3.2 Tissue Setup

In order to test the accuracy of electrogram mapping over a variety of activation frequencies, virtual tissues were created with heterogeneous physiologic parameters. Each tissue was made up of 6400 cells (80x80mm^2) to provide sufficient tissue area to support MWR. To generate heterogeneity in the activation frequency, a Gaussian filter was applied to an array (80x80) with a random distribution of values to create smooth gradients between regions of higher and lower APDs (Range 60-100ms). Local APD heterogeneity was programmed into the tissue ($\pm$10ms). Intercellular resistance remained constant in all tissues (11Ω).

4.3.3 Electrogram Recordings

As shown previously [4, 5], the accuracy of electrogram frequency mapping is dependent on both the size of the electrode and the configuration used (unipolar<contact bipolar<orthogonal close unipolar (OCU)) to generate electrograms. Therefore, we sought to create an electrode shape that would allow near OCU-like recordings independent of its rotation with the tissue plane. At each recording location, four electrodes were made up of the quadrants of a cylinder positioned on its side.

Each electrode was created using a finite element mesh (20 elements per electrode); electrogram calculations were described previously [4]. Electrogram recordings were made from an 8x8 array of evenly spaced recording sites.

4.3.4 Analysis

MWR was induced by burst pacing (20ms cycle length for 1 second) from random locations within the tissue. Electrograms and cell voltages were collected during 10s of MWR. Action potential times were detected at each cell and cycle lengths between activations were identified. Tissue activation frequency (TF) was calculated as the inverse of the average cycle-length during the recorded 10s episode of MWR.

At each electrode recording location, the electrode closest to the tissue was identified by the electrogram with the highest magnitude of its time derivative (sharpest peaks). Bipolar electrograms were created at each location using the electrogram of the contact electrode and its opposite pair. Bipolar electrograms were then filtered using a low pass filter (75Hz cutoff frequency) to remove high frequency noise. Peaks were identified using the zero crossings of the time derivative of the electrogram signal. Electrogram frequency was then calculated as the inverse of the average cycle length between identified peaks at each recording location.

As shown previously [6], spatiotemporal variability of a tissue can change over time causing fractionated events if electrode spatial resolution is inadequate. Therefore, a filter was created to remove confounding effects by fractionation on the calculated electrogram frequency. Cycle lengths between peaks that were identified as less than 25ms were considered fractionated events and were removed from the frequency calculation.

We hypothesized that the height of an electrode could be identified using only the characteristics of its electrogram signal. Unipolar electrograms from 10s of MWR were filtered with a low pass filter (75 Hz cutoff frequency) and the time derivative of each signal was taken. The peak amplitude of the electrogram derivative (dV/dt) was identified for each action potential. The 20 highest peaks were then averaged to exclude electrogram potentials from far-field sources. We calculated the difference of the peak dV/dt (delta dV/dt) between each electrode and its opposite electrode within a pair. The electrode pair with the lower difference in peak dV/dt at each recording location is discarded.

4.3.5 Impact of electrode position on frequency and accuracy

We investigated the effect of electrode distance from the tissue and its rotation with respect to the tissue plane on the electrogram frequency and its accuracy (with respect to TF). Electrode height (distance from tissue) was varied from tissue contact to 8mm (2mm intervals) from the tissue surface. For each electrode height, electrode rotation was varied between 0° and 90° (15° intervals). Electrograms and TF were calculated in ten different tissues with 10 initiations of MWR per tissue for each electrode height and rotation. The delta dV/dt and correlation coefficient were calculated between TF and electrogram frequency for each electrode height and rotation. We identified the delta dV/dt threshold above which electrode height was less than 2mm.

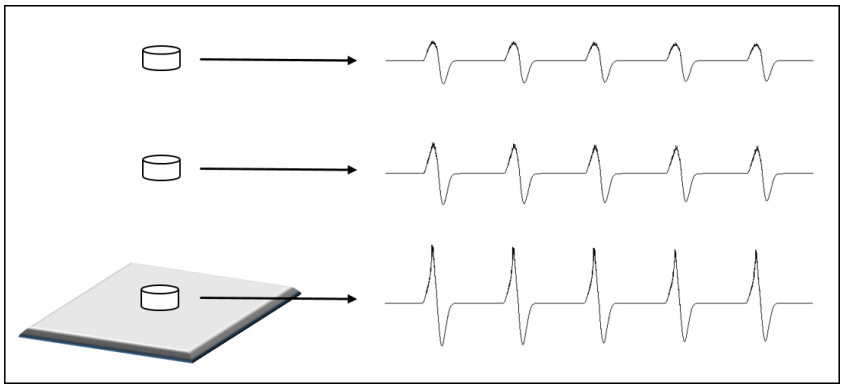

Figure 4.1: Impact of the electrode distance to the tissue on the morphology of the electrogram generated from tissue activation passing by the recording region. Both signal amplitude as well as sharpness are affected by increasing the distance of the recording electrode from the potential source.

4.3.6 Impact of electrode spatial resolution on frequency and accuracy

In order to investigate the effect of fractionation on the electrogram frequency and accuracy (with respect to TF), the spatial resolution of electrodes was altered by increasing the electrode size. Electrode radius was varied between 1mm and 5mm (1mm interval) while electrode length was varied between 2mm and 10mm (2mm interval). Electrograms and TF were calculated from five tissues with ten episodes of MWR per tissue. The number of fractionated events was identified from each episode of MWR by counting the number of inter-potential cycle lengths less than 25ms. The correlation between electrogram frequency and TF was calculated for each electrode size before and after filtering out fractionated events.

4.3.7 Effectiveness of delta dV/dt to identify tissue contact

To validate the efficacy of the electrode height identification with delta dV/dt, we simulated a clinical environment where both the orientation and the distance from the tissue surface of an electrode are unknown. Electrode heights were selected from a gamma distribution (k=2, θ=1) to generate a larger sample size of near-tissue electrograms. Electrode rotations were randomly selected from a normal distribution (μ=θ, σ=15°). Electrograms and TF were calculated from ten episodes of MWR per tissue in ten tissues. Electrogram frequency was then calculated with fractionation effects removed. Delta dV/dt was identified at all recording locations (8x8 array of evenly spaced electrodes). Correlation coefficient was calculated between TF and EF at 1) all recording locations, 2) locations whose delta dV/dt $>$ 0.02, and 3) locations at which electrode distance from the tissue $<$ 2mm.

4.3.8 Biologic Validation

In four swine, access to the left atrium was gained through a left lateral thoracotomy. MWR was induced via burst pacing on the epithelial surface of the left atrium. In order to increase the propensity and duration of MWR events, the vagus nerve was stimulated with 2-5V at 10Hz. During both sinus rhythm and MWR, electrograms were collected epicardially using a stacked electrode catheter placed orthogonally to the tissue surface. Electrogram delta dV/dt was assessed for each electrogram as described above.

4.4 Results

4.4.1 Electrogram frequency as a function of height

In simulated data of multi-wavelet reentry, electrogram frequency decreased exponentially as a function of increasing height. Correlation to activation frequency was highest at tissue contact ($r^2 = 0.97$) and dropped rapidly when electrode distance to the tissue surface exceeded 2mm. Electrogram frequency similarly decreased with increasing electrode height *in vivo*. The degree by which electrogram frequency decreased was a function of the frequency of atrial fibrillation. During lower frequency AF (7Hz), the difference in electrogram frequency observed between contact and noncontact electrodes was 0.4 ± 0.1 Hz. On the contrary, during higher frequency AF (9Hz), the difference in observed electrogram frequency varied by 2Hz between contact and non-contact electrodes.

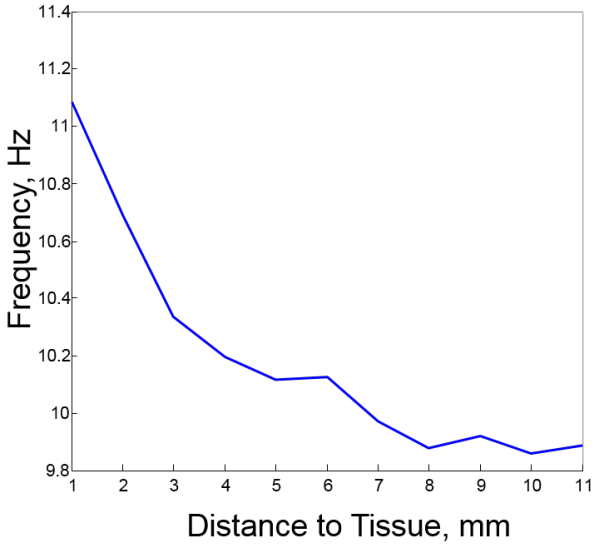

Figure 4.2: Assessment of unipolar electrogram frequency as a function of electrode distance to the tissue surface. The range of frequencies observed due to changes in electrode height are on the same order as frequency differences due to heterogeneous physiologic parameters in the tissue addressing the importance of tissue-contact electrogram mapping.

4.4.2 Delta dV/dt as a function of electrode height and rotation

In simulated as well as induced AF in pigs, the magnitude of electrogram delta dV/dt fell off exponentially as a function of both electrode height and rotation from an orthogonal axis (Figure 4.3). The correlation between tissue frequency and electrogram frequency weakened as a function of both electrode distance from the tissue and the orientation of the electrode configuration. However, for electrode heights $\leq$2mm and electrode rotation $<30^{\circ}$ from the orthogonal axis, correlations remained

relatively constant ($r^2 = \pm 0.05$). The delta dV/dt threshold was therefore selected by identifying the delta dV/dt where electrode height was equal to 2mm (0.02).

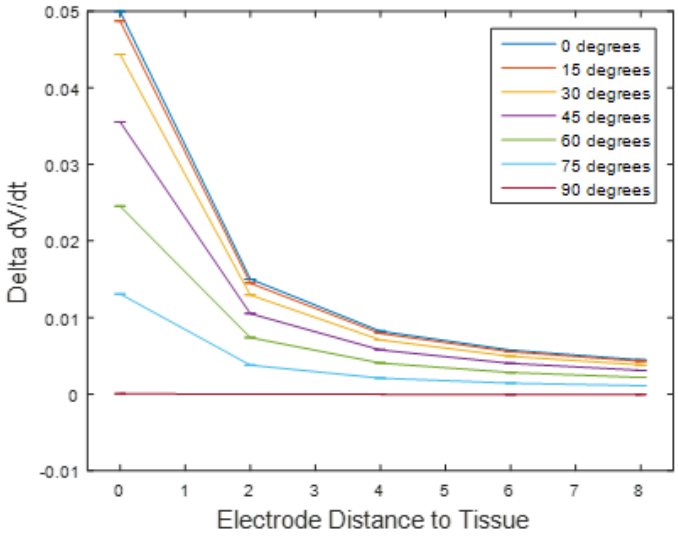

Figure 4.3: Assessment of electrogram derived metric as a tool to identify tissue contact and rotation. The magnitude of delta dV/dt is shown as a function of both electrode distance to the tissue (x-axis) and rotation away from an orthogonal electrode configuration. Due to the dissociation of electrogram frequency and activation frequency for distances greater than 2mm and bipolar rotations greater than 30 degrees, a cutoff threshold of 0.02 was chosen.

4.4.3 Effect of filtering fractionated events

The mean number of fractionated events identified per episode of MWR increased linearly with increasing electrode size (decreased spatial resolution). Accordingly, correlation between tissue frequency and electrogram frequency decreased linearly as electrode size increased. The number of fractionated events varied significantly between episodes of MWR. The coefficient of variation of fractionated events ranged

from 0.34 with the largest electrode to 0.68 with the smallest electrode. This suggests that fractionated events were not temporally stable and the spatial complexity of the tissue varied over time. After the application of the filter to remove fractionated events from the electrogram frequency measurement, correlation to tissue frequency improved ($r^2 = 0.90$ vs 0.82, $p < 0.05$) and the rate of correlation decay decreased with increasing electrode size (-0.007 per mm radius vs. -0.012 per mm radius).

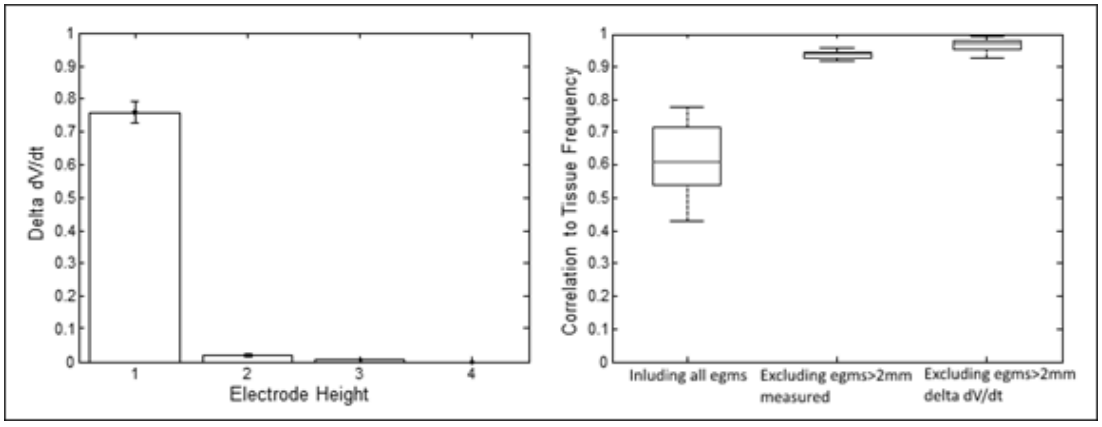

Figure 4.4: Relationship between delta dV/dt and electrode distance to the tissue collected during induced AF in swine (Left). Correlation between electrogram frequency and activation frequency with random distribution of electrode heights, using only electrograms whose delta dV/dt exceeds a contact threshold, and electrograms generated from electrodes with distance to the tissue < 2mm (Right).

4.4.4 Efficacy of delta dV/dt to identify tissue contact

Following randomization of electrode orientation and distance from the tissue surface, overall correlation of electrogram frequency to tissue frequency was 0.61 (r^2)

and was highly variable (SEM=0.036). Using the electrogram derived filter, frequency correlation increased to 0.94 and the range of correlations stabilized (SEM=0.004). To compare the success of the algorithm to the physical height of the electrodes, using only electrodes whose distance from the tissue surface exceeded 2mm increased the correlation to tissue frequency to 0.96±0.007.

4.5 Discussion

In order to develop a more successful strategy for the treatment of atrial fibrillation, one must explore the substrate responsible for the perpetuation of AF. As with all arrhythmias, unless current is continuously being supplied to the tissue, continuous activation requires re-excitation by existing waves within the tissue. In its most organized form, this would take the shape of either structural reentry around an existing boundary or scar tissue or a stable rotating wave around a functional boundary. In MWR, we find the path traveled by a reentrant wave is not stable and multiple reentrant waves can exist in the tissue at any given time. Similar to the termination of a structural reentrant wave, successful ablation of spatially unstable reentrant waves requires the complete transection of the wave-front. It is, therefore, necessary to identify the center of rotation of these waves, or circuits, for complete termination. We have previously demonstrated a method for the identification of circuits in MWR [7]. Briefly, a circuit is defined by the enclosed area circumscribed by a rotating wave-end which is unattached to a tissue boundary. It was shown that linear ablation guided by the distribution of circuits was more effective than both random ablation and baseline duration.

The precise tracking of waves clinically is challenging with current technologies. We discovered that the circuit density distribution correlated inversely with the local wavelength of the tissue [2]. The presence of MWR in a tissue with a heterogeneous distribution of wavelength causes a shifting conduction block in regions with slower repolarization times. We postulated that regions of tissue responsible for driving MWR would be activated more frequently, while regions being passively activated would have instances of conduction block, therefore, reducing its activation frequency. Our data gathered in computer simulations supported our hypothesis; tissue activation frequency correlated with circuit density over a wide range of conditions.

While the use of tissue activation frequency proved to be an effective surrogate for the identification of reentrant drivers in MWR, one cannot directly measure its frequency. An electrode measures the distance weighted current density of all cells in the heart. As such, an electrogram is not a measure of an individual myocyte, but rather a region of tissue whose size is dependent on the spatial resolution of the electrode. We previously demonstrated that electrogram frequency inaccurately identifies tissue frequency when the spatial resolution of the electrode causes the simultaneous mapping of multiple dissociated muscle fibers [4]. Therefore, electrogram frequency only reflects tissue frequency when the spatial resolution of the electrode is sufficient to record a synchronously activated region of tissue. Previous data showed that the accuracy of electrogram frequency improved with increasing spatial resolution [5] (orthogonal close unipolar>contact bipolar>unipolar).

One might expect that by raising the electrode farther from the tissue surface, it would create the potential to observe multiple wave events thereby increasing its chance to overestimate the local activation frequency similar to the effect of using

a larger electrode or an electrode configuration with lower spatial resolution. We find, however, that in the process of increasing the distance to the tissue, electrogram potentials begin to blend with each other. The result of which causes undercounting in the electrogram frequency measurement. The degree to which this occurs is on the same order as the tissue frequency varies due to its heterogeneous properties (APD, resistance) emphasizing the importance of electrode-tissue contact. Clinically, the position of an electrode relative to the tissue surface is difficult to validate. We, therefore, sought to develop an electrogram derived metric to assess the distance of a recording electrode to the tissue surface.

We hypothesized that electrogram sharpness best identifies electrode proximity to the tissue surface. With unipolar electrodes, sharpness can also be affected by changes in wave conduction velocity and the presence of wave collisions within the recording region. However, using the relative difference in sharpness between two electrodes oriented orthogonally to the tissue plane enhances its relationship with distance to tissue (difference in sharpness falls off more quickly with increasing distance) while reducing the impact of conduction velocity and wave collision. Our data suggests, in both *in silico* and *in vivo* settings, that the difference in electrogram sharpness can be used to identify electrode proximity to the tissue surface.

As described in our previous paper [2], the accuracy of electrogram frequency mapping is dependent on the spatial resolution of the recording site. We showed that electrograms generated from an orthogonal electrode configuration were more accurate that a parallel orientation. This is the result of both the directional dependence of waves approaching the parallel recording site as well as having lower spatial resolution compared to an orthogonal configuration. Similar to electrode distance to

the tissue surface, the orientation of a catheter with respect to the tissue is clinically difficult to validate. However, by comparing the electrogram sharpness for each of the unipolar electrodes making up the bipolar configuration, one can gain insight on its rotation with respect to the tissue surface. We find that the difference in electrogram sharpness between the unipolar electrodes is greatest in an orthogonal configuration and approaches zero as the angle approaches a parallel configuration. This suggests that electrogram sharpness can be used not only to identify electrode distance to the tissue but also to assess its orientation relative to the tissue plane.

Fractionation in electrograms has been an area of interest in the identification of ablation sites for complex fractionated atrial electrogram (CFAE) mapping [8, 9, 10, 11, 12]. Algorithms for the detection of CFAE sites typically involve the detection of multiple peaks per activation in an electrogram or a short average cycle length (<80ms). Observing multiple peaks per activation can be the result of having electrodes with an insufficient spatial resolution to dissociate independent wave events in the recording region of the electrode. This information can be useful as this will likely identify sites of focal firing events but can also be the result of wave collisions or simultaneous passive activation through the tissue and conduction fibers. By classifying a region of tissue to be continuously fractionated with a cycle length $<$ 80ms, one must assume that continuous activation at this rate is not physiologically viable during AF. If on the other hand, the tissue is capable of supporting this rate during AF, this form of CFAE mapping becomes the identification of high-frequency sites in the tissue which is the premise of frequency mapping. In this paper, we define a 'fractionation filter' by declaring cycle lengths to be physiology inviable under 25ms in order to remove activations involving multiple peaks which are likely to be

caused by electrodes with insufficient spatial resolution. In doing so, we find that the accuracy of electrogram frequency to tissue frequency improves. The degree to which the filter improves its accuracy is dependent on the spatial resolution of the electrode. For larger electrodes, spatial resolution decreases and we observe more fractionated events in electrograms. Therefore, the fractionated filter improves the accuracy to a larger degree than electrodes with higher spatial resolution.

4.5.1 Limitations

As is the case with all experiments relying heavily on computational modeling, many of these findings will need to be validated in a biological system. While we were able to validate the effect of increasing electrode distance to the tissue on the sharpness of the electrogram in swine, the use of computational models was required to accurately identify tissue frequency and make correlations to electrogram frequency under various electrode positions and orientations. Electrode size and morphology could be modified immediately without long wait times for fabrication of new catheters. Computational simulations also permitted complete control over physiologic parameters such as action potential duration and intercellular resistance to vary both the rate and complexity of wave events. This along with the high throughput nature of our computational model allowed us to investigate our hypotheses over a wide spectrum of MWR quickly.

4.6 Conclusions

The accuracy of electrogram frequency mapping is dependent on both the spatial resolution of the recording electrode as well as its position and relative orientation to the tissue plane. While the spatial resolution of an electrode can be permanently affected through the use of a bipolar configuration or by changing its size, the morphology and distance to the surface of the heart are largely unknowns. Our data suggests that one can use a signature of an electrogram to assess both the electrode proximity to the tissue surface and its orientation.

Although fractionation can have a large impact on the accuracy of electrogram frequency mapping, we found that it can be largely mitigated through the use of higher resolution electrodes as well as providing a filter eliminating very short cycle length events (multiple peaks per activation). Each of these effects increased the correlation of electrogram frequency to tissue activation frequency. Further work will be required to assess the degree of fractionated events in a biological model as it has a more complex conduction system than our computational simulations. While we have shown adequate spatial resolution of our electrode design in a swine model of AF, a clinical study will be required to identify the range of spatial complexities seen in human patients to evaluate if the spatial resolution of our electrode design is sufficient.

Bibliography

[1] P. S. Spector et al. "Ablation of multi-wavelet re-entry: general principles and in silico analyses". In: *Europace* 14 Suppl 5 (2012), pp. v106–v111.

[2] B. E. Benson et al. "Mapping multi-wavelet reentry without isochrones: an electrogram-guided approach to define substrate distribution". In: *Europace* 16 Suppl 4 (2014), pp. iv102–iv109.

[3] Peter S. Spector et al. "Emergence of Complex Behavior: An Interactive Model of Cardiac Excitation Provides a Powerful Tool for Understanding Electrical Propagation". In: *Circulation: Arrhythmia and Electrophysiology* (2011).

[4] J. M. Stinnett-Donnelly et al. "Effects of electrode size and spacing on the resolution of intracardiac electrograms". In: *Coron Artery Dis* 23.2 (2012), pp. 126–32.

[5] N. C. Thompson et al. "Improved spatial resolution and electrogram wave direction independence with the use of an orthogonal electrode configuration". In: *J Clin Monit Comput* 28.2 (2014), pp. 157–63.

[6] D. D. Correa de Sa et al. "Electrogram fractionation: the relationship between spatiotemporal variation of tissue excitation and electrode spatial resolution". In: *Circ Arrhythm Electrophysiol* 4.6 (2011), pp. 909–16.

[7] R. T. Carrick et al. "Ablation of multiwavelet re-entry guided by circuit-density and distribution: maximizing the probability of circuit annihilation". In: *Circ Arrhythm Electrophysiol* 6.6 (2013), pp. 1229–35.

[8] M. Chen et al. "Randomized comparison between pulmonary vein antral isolation versus complex fractionated electrogram ablation for paroxysmal atrial fibrillation". In: *J Cardiovasc Electrophysiol* 22.9 (2011), pp. 973–81.

[9] Sanjay Dixit et al. "Randomized Ablation Strategies for the Treatment of Persistent Atrial Fibrillation: RASTA Study". In: *Circulation: Arrhythmia and Electrophysiology* 5.2 (2012), pp. 287–294.

[10] C. S. Elayi et al. "Ablation for longstanding permanent atrial fibrillation: results from a randomized study comparing three different strategies". In: *Heart Rhythm* 5.12 (2008), pp. 1658–64.

[11] Karen T.S. Konings et al. "Configuration of Unipolar Atrial Electrograms During Electrically Induced Atrial Fibrillation in Humans". In: *Circulation* 95.5 (1997), pp. 1231–1241.

[12] Koonlawee Nademanee et al. “A new approach for catheter ablation of atrial fibrillation: mapping of the electrophysiologic substrate”. In: *J Am Coll Cardiol* 43.11 (2004), pp. 2044–2053.

Chapter 5

Neural Network for the Real-Time Classification of Activation Patterns in Atrial Fibrillation

Bryce E Benson, BS^{1}, Richard Carrick, $BS^{1,2}$, Jason HT Bates, PhD, $DSc^{1,2}$, and Peter Spector, MD^{2}

[1]University of Vermont College of Mathematics and Engineering, Burlington, VT;

[2]University of Vermont College of Medicine, Burlington, VT

5.1 Abstract

Introduction: We recently demonstrated that electrogram frequency mapping using high resolution electrodes can identify circuit core distribution in multi-wavelet reentry. High frequency sites are not unique to multi-wavelet reentry; they can also be produced by focal drivers (triggered firing or stable rotors). Ablation strategy may vary depending upon the underlying substrate. After identifying high frequency regions, it would be ideal if local multi-electrode recordings could reveal their underlying mechanism. We developed a real-time automated tool to distinguish driver type.

Methods: In computational modeling, stable rotors, concentric activation, and passive linear activation were generated. Virtual electrograms were calculated from locations

resembling a Pentaray catheter (5 splines/3 electrodes per spline). Activation times were identified in 100ms windows and normalized to be used as inputs for a counter-propagation neural network. 3600 examples of concentric activation, rotational waves, and linear activation were used in training the network for classification of activation patterns.

Results: Following training of the neural network, 897 of 900 randomized activation patterns were successfully classified. The computational efficiency of our algorithm allows real-time classification of activation patterns, making it potentially useful for clinical mapping.

Conclusions: The activation pattern of a driver in AF influences the appropriate ablation strategy. Real-time pattern recognition can be achieved via a neural network with simultaneous multi-electrode recordings.

5.2 Introduction

Atrial fibrillation (AF) is the most common cardiac arrhythmia and can be described as the chaotic motion of electrical waves throughout the atria. This irregular behavior contributes to a large burden on cardiac health. Despite its prevalence and complications, treatments have remained problematic both pharmacologically and surgically [1]. Catheter ablation is a minimally invasive surgical treatment of AF which involves guiding wires into the heart through a vein in the arm, groin, or neck. Radiofrequency energy is then applied through the wires to destroy regions of tissue in the atria as a means to disrupt the chaotic electrical behavior. Traditional catheter ablation involves the elimination of potential trigger sites and has shown moderate

success in patients with early onset (paroxysmal) AF, but success rates diminish in more progressed forms of the disease. This is largely due to its failure to identify the substrate responsible for the perpetuation of arrhythmia.

We recently demonstrated that electrogram frequency mapping using high-resolution electrodes can identify circuit core distribution in multi-wavelet reentry, a form of AF consisting of multiple spatially unstable wavelets causing perpetual arrhythmia [2]. In computer simulations, ablation guided to high-frequency regions caused a significant reduction in the duration of fibrillation compared to blind ablation [3].

High-frequency sites are not unique to multi-wavelet reentry, but can also be produced by focal drivers [4]. Focal drivers can take the form of triggered firing (concentric activation) or spatially stable rotors. Ablation of focal drivers is imperative for successful treatment; however, the technique of intervention required is dependent on the form of driver. Simultaneous multi-electrode recordings in the high-frequency area of interest could reveal the underlying mechanism. We, therefore, developed a real-time automated tool to distinguish driver type using electrogram activation timings and assessed its ability to correctly classify activation patterns.

5.3 Methods

In order to develop a tool for the classification of focal drivers during AF, the true activation pattern must be known. In a biological setting, recreating an activation map is difficult to achieve without high-density electrode arrays with sufficient spatial resolution. We, therefore, used a computational model of excitable media to allow complete visibility of the activation pattern as well as control over electrode design

and placement [5].

Activation patterns of stable rotors (clockwise and counter-clockwise rotation), concentric activation, and passive linear activation were simulated in a computer model of excitable media. The model consists of a grid of two-dimensional excitable 'cells', each representing a group of myocytes. Cells are electrically connected to their neighbors (Von Neumann neighborhood) via resistive pathways and exchange current according to their voltage difference and intercellular resistance. Upon exceeding a threshold voltage, cells exhibit a simulated action potential whose morphology is dependent on intrinsic behavior (upstroke time, plateau time, repolarization time) as well as extrinsic current exchanges with neighboring cells.

Virtual electrograms were calculated simultaneously, as described previously [6], from a multiple electrode catheter design during each activation pattern. The catheter consisted of five splines, with three electrodes per spline at 2, 6, and 10 mm radial distance from the center of the catheter. The catheter center was varied with respect to the center of focal drivers in each scenario to account for activation timing discrepancies when the catheter was not centered on the activation pattern. Electrode positions and the flowchart for activation pattern classification is shown in figure 5.1

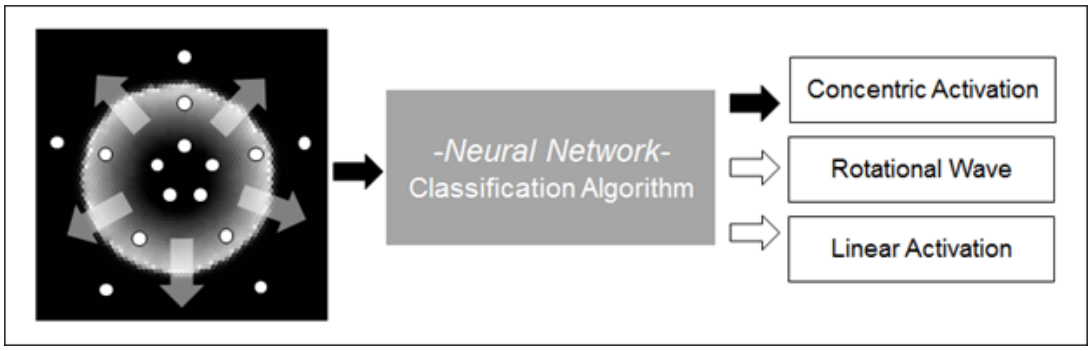

Figure 5.1: Flowchart for the classification of activation patterns using a neural network. Electrode position is shown centered over a concentric activation pattern.

A counter-propagation style neural network [7] was chosen to classify the electrogram signals into an activation pattern. In order to translate the electrogram signals into a usable input to the neural network, the time series was split up into 100ms segments. Activation times were identified as the time index for each peak in the electrogram signal. If no peak appeared for an electrode within a 100ms window, the maximum time (100ms) was assigned. In the case of two peaks occurring within the same time segment, the first peak was chosen.

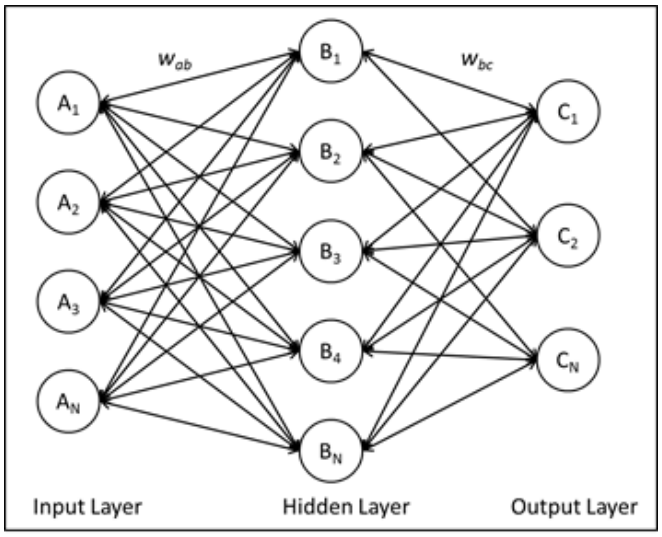

Figure 5.2: Visual representation of the classification algorithm used to identify activation patterns using electrograms. Normalized activation times within a 100ms window from the 15 electrogram signals are treated as inputs to the system. Outputs correspond to the classified activation pattern assigned by the trained weights between layers.

The activation times for each electrode in a given window were then normalized to their combined Euclidean distance and used as inputs to the network. Because the relative positions of the electrodes with respect to each other remains unchanged, location data was omitted as an input to the network. Initial Kohonen (1st to 2nd layer) weights to the 5,000 node hidden layer as well as Grossberg weights (2nd to 3rd layer) were initially randomized and normalized to their combined Euclidean distance. The output layer was limited to three classifications: stable rotors, concentric activation, and passive linear activation.

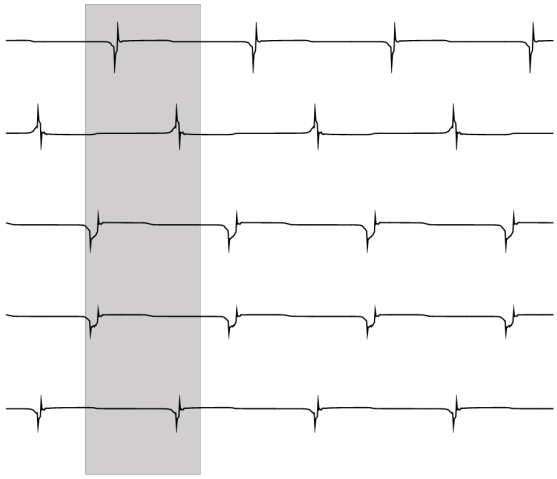

Figure 5.3: Simulated electrograms generated from five locations within the multi-electrode catheter. The gray rectangle denotes a window of time to identify the electrogram activation times. These activation times are then normalized and fed into the neural network (from all 15 locations) and are then classified into an activation pattern.

Kohonen layer values were calculated as the dot product between inputs and weights to a given node. The node with the highest dot product was selected as the winner and all weights connected to it were updated as shown in equation 5.1 below.

$$W_{ij}^{'} = W_{ij} + a * (P - W_{ij}) \tag{5.1}$$

Where W_{ij} are the previous weights attached to the winning node j, a is the learning coefficient to the Kohonen layer (0.7), and P is the current training pattern. The winning node from the hidden layer was then activated and set to one while all other nodes are eliminated. Finally, the Grossberg weights are updated from the winning Kohonen node to match its associated activation pattern as shown below.

$$W_{jk}^{'} = W_{jk} + b * (T - W_{jk}) \tag{5.2}$$

Where W_{jk} are the previous weights from the winning node j, b is the learning coefficient for the Grossberg layer, and T is the correct classification to the current training pattern.

Training success was evaluated during each iteration using the root mean square error (RMSE) between the assigned classification at the given iteration and the true activation patterns. The network was allowed 200 iterations for the weights to converge. Following training, the network was evaluated via an interpolation set of 600 additional patterns consisting of each of the three classifications. The robustness of the network to slight perturbations in the activation times was evaluated by a applying white noise filter with amplitude up to 10% of the activation time.

5.4 Results

In the training phase, 1200 examples of stable rotors, concentric activation, and passive linear activation were created (3600 total). Network weights converged within 50 iterations with an RMSE of 0.015 (Figure). Following 200 iterations of training, 99.94% (3,598 of 3,600) training patterns were successfully classified.

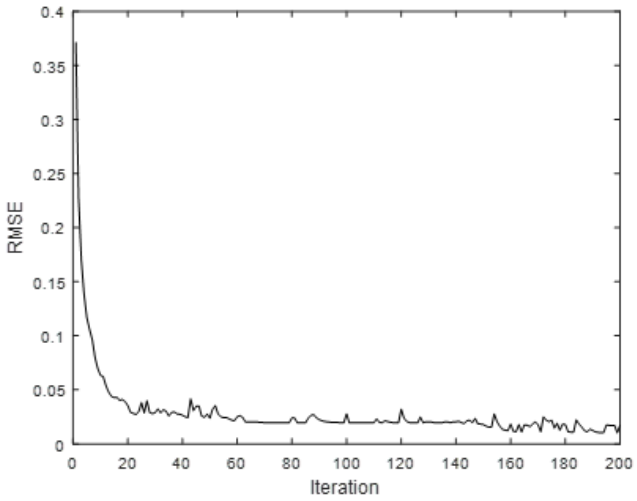

Figure 5.4: Root mean square error (RMSE) as a function of the number of training iterations. Convergence is observed within 50 iterations of training.

An interpolation set of 900 additional patterns was created in the computational model (300 of each classification) to evaluate the network using an untrained series of data. The network successfully classified 99.7% (897 of 900) of the untrained activation patterns. Following the addition of a white noise filter to evaluate the robustness of the neural network to random small changes in the input patterns, 95.1% (856 of 900) input patterns were successfully classified.

In addition to its ability to successfully classify activation patterns, the network is computational efficient (0.003s) in classifying additional patterns. This makes it a viable tool for real-time classification of activation patterns in a clinical mapping scenario.

5.5 Discussion

A successful ablation strategy for atrial fibrillation requires a complete depiction of the substrate responsible for its perpetuation. The limited success of traditional catheter ablation is largely due to the blind approach it takes by eliminating potential trigger sites in the pulmonary veins. Using computer modeling we have the ability to study the excitation of every cell and make inferences about the driving forces causing the maintenance of AF. Depending on the collective properties of the underlying tissue, atrial fibrillation can take a number of different forms. In its simplest form, perpetuation is caused by a single stable rotating wave that can spawn daughter wavelets causing fibrillatory conduction outside its direct area of influence. In this scenario, elimination of the rotor terminates the arrhythmia as the surrounding tissue is unable to maintain the arrhythmia. Decreasing the excitability of the tissue destabilizes the single rotor causing it to meander; however, its elimination leads to the quiescence of the tissue. In its most chaotic form, multi-wavelet reentry (MWR), multiple spatially unstable rotating waves are responsible for the perpetuation of the rhythm and only when all of these driving forces are eliminated does MWR cease to perpetuate. Separate from reentrant based arrhythmias, AF can also be maintained by regions of tissue spontaneously depolarizing known as focal firing. These mechanisms manifest similarly to focal rotors in that they are typically spatially stable and cause fibrillatory conduction further from the source.

The successful treatment of AF is contingent on distinguishing the substrate responsible for its perpetuation. In the case of a reentrant arrhythmia (rotors and MWR), only ablation lesions which completely transect a rotating wave from an

outer boundary to its core will cause termination. In MWR and meandering rotors, this involves the placement of lesions based on the probability distribution of where rotor cores are most likely to occur [8]. Conversely, successful ablation of a focal firing mechanism simply requires the elimination of spontaneously depolarizing cells [9]. Although the primary goal of ablation therapy is to restore sinus rhythm to the heart, lesions placed will permanently block conduction pathways and inhibit some of the mechanical function of the atria. It is, therefore, necessary to optimize the placement and strategy of ablation lesions such that sinus rhythm is restored while preserving the mechanical function of the atria.

In a clinical setting, our understanding of the underlying mechanism is convoluted. Intracardiac electrograms provide us with insight on the local current density in a region of tissue. The accuracy of electrograms with respect to cellular excitation is dependent on the spatial resolution of the electrode as well as its proximity to the tissue [10]. However, using electrograms to map the activation sequence in the atria is not clinically viable due to the electrode sampling requirements to recreate its chaotic behavior. We previously demonstrated that local tissue activation frequency and electrogram frequency, provided adequate spatial resolution, correlated with the distribution of rotor cores in MWR [2]. Similarly, frequency mapping can be used to localize stable rotors and focal firing to their region of 1:1 conduction as they are driving the arrhythmia and thus activating faster than other regions [4, 11].

Although electrogram frequency mapping is able to identify the area of interest for a successful ablation, it is unable to distinguish between reentry and focal firing mechanisms. Activation mapping was previously mentioned to be inviable in AF due to the constraints on sampling and the size of the tissue. However, when used in

conjunction with frequency mapping to focus on an area of interest, we hypothesized that high-density simultaneous electrogram recordings could be used to reveal the underlying mechanism. To be used viably in a clinical setting, mechanism classification should be accomplished real-time and not subject to a human interpretation of electrograms. We, therefore, reasoned that a neural network trained on activation patterns from reentrant arrhythmias, focal firing, and passively driven tissue could be used as a tool to classify activation patterns real-time.

The counter-propagation network was first introduced by Hecht-Nielsen [7]. This network combined the architecture of the self-organizing map by Kohonen [12] and the outstar structure by Grossberg. The network was chosen in this scenario for its ability to classify patterns efficiently as well as its ability to handle continuous vector inputs. In order to reduce the dimensionality of electrograms to be fed into the neural network as inputs, activation times were identified at peaks in the electrograms for each location. The signals were then segmented into 100ms windows to investigate the pattern of a single activation as it passes through the area of interest. In order to prevent bias in the training phase, the vector of activation times was normalized by their Euclidean length. The number of nodes in the Grossberg (hidden) layer of the network was chosen according to the number of patterns used in training the network with additional included to envelope a larger percent of the state space. Initial Kohonen and Grossberg weights were initially randomized due to the absence of large clusters of input vectors in the training patterns. The rapid convergence of weights as shown in the RMSE curve after 50 iterations suggested the representation of electrograms as activation times was adequate for classification into driver types. We demonstrated the accuracy of the neural network with an interpolation set of 900

additional patterns which were correctly classified in 99.7% of the patterns.

5.5.1 Limitations

A computational model of excitation was used in the creation of activation patterns as well as electrogram generation. In order to be clinically viable, an interpolation set including activation patterns collected from a biological system will ultimately be required. The network was also trained for a specific electrode layout with the assumption that the position of electrodes relative to each other remained unchanged. Intracardiac catheters are designed to have pliable splines to maneuver themselves into the heart and make contact with the tissue surface. The compliance of this catheter design must be investigated to ensure this assumption holds. Otherwise, an alternative catheter design in which electrodes are rigidly held on a flat plaque could be trained on the network to ensure their relative positions to each other remains constant.

5.6 Conclusion

Recent mapping strategies for atrial fibrillation have begun to take a targeted approach to identifying the substrate responsible its perpetuation. We have previously demonstrated that electrogram frequency mapping can be used to identify regions of tissue responsible for driving the arrhythmia. Classification of the driving mechanism is required to develop an optimized ablation strategy and minimize unnecessary lesions. Electrogram frequency guided activation mapping can provide insight on the driving mechanism. We developed a neural network to distinguish the underly-

ing mechanism in the high frequency area using the relative activation times from a multi-electrode recording.

Bibliography

[1] C. T. January et al. "2014 AHA/ACC/HRS guideline for the management of patients with atrial fibrillation: executive summary: a report of the American College of Cardiology/American Heart Association Task Force on practice guidelines and the Heart Rhythm Society". In: *Circulation* 130.23 (2014), pp. 2071–104.

[2] B. E. Benson et al. "Mapping multi-wavelet reentry without isochrones: an electrogram-guided approach to define substrate distribution". In: *Europace* 16 Suppl 4 (2014), pp. iv102–iv109.

[3] P. S. Spector et al. "Ablation of multi-wavelet re-entry: general principles and in silico analyses". In: *Europace* 14 Suppl 5 (2012), pp. v106–v111.

[4] Omer Berenfeld et al. "Spatially Distributed Dominant Excitation Frequencies Reveal Hidden Organization in Atrial Fibrillation in the Langendorff-Perfused Sheep Heart". In: *J Cardiovasc Electrophysiol* 11.8 (2000), pp. 869–879.

[5] Peter S. Spector et al. "Emergence of Complex Behavior: An Interactive Model of Cardiac Excitation Provides a Powerful Tool for Understanding Electrical Propagation". In: *Circulation: Arrhythmia and Electrophysiology* (2011).

[6] D. D. Correa de Sa et al. "Electrogram fractionation: the relationship between spatiotemporal variation of tissue excitation and electrode spatial resolution". In: *Circ Arrhythm Electrophysiol* 4.6 (2011), pp. 909–16.

[7] R. Hecht-Nielsen. "Counterpropagation networks". In: *Appl Opt* 26.23 (1987), pp. 4979–83.

[8] R. T. Carrick et al. "Ablation of multiwavelet re-entry guided by circuit-density and distribution: maximizing the probability of circuit annihilation". In: *Circ Arrhythm Electrophysiol* 6.6 (2013), pp. 1229–35.

[9] Sanjiv M. Narayan et al. "Treatment of Atrial Fibrillation by the Ablation of Localized Sources: CONFIRM (Conventional Ablation for Atrial Fibrillation With or Without Focal Impulse and Rotor Modulation) Trial". In: *J Am Coll Cardiol* 60.7 (2012), pp. 628–636.

[10] J. M. Stinnett-Donnelly et al. "Effects of electrode size and spacing on the resolution of intracardiac electrograms". In: *Coron Artery Dis* 23.2 (2012), pp. 126–32.

[11] Felipe Atienza et al. “Real-time Dominant Frequency Mapping and Ablation of Dominant-Frequency Sites in Atrial Fibrillation with Left-to-Right Frequency Gradients Predicts Long-Term Maintenance of Sinus Rhythm”. In: *Heart Rhythm* 6.1 (2009), pp. 33–40.

[12] Teuvo Kohonen. “Self-organized formation of topologically correct feature maps”. In: *Biological Cybernetics* 43.1 (1982), pp. 59–69.

Chapter 6
Conclusion

Atrial fibrillation continues to be a growing problem in our healthcare system today despite seemingly immeasurable amounts of money, time, and manpower given in search for a cure. While numerous research groups have developed effective strategies for treating patients with early onset disease, patients with the highest disease burden remain refractory to all modern methods of treatment. In part, this is the result of our failure to grasp that the mechanism for AF perpetuation may exist in multiple forms. Existing mapping and ablation strategies are tailored to a specific mechanism which will ultimately fail upon encountering alternative forms of AF.

Since the discovery of ectopic foci in the pulmonary veins which ushered our modern standard of care for ablation of AF (pulmonary vein isolation), the emphasis has shifted away from the multiple wavelet theory as the primary mechanism for the perpetuation of atrial fibrillation. However, high-resolution multi-site electrode mapping studies have recently shown multi-wavelet reentry (MWR) is commonly observed in patients with various levels of disease burden. Identification of the substrate responsible for the perpetuation of MWR using clinically available means has yet to be thoroughly investigated. Here, a substrate guided mapping strategy is proposed built on findings that show ablation guided by the distribution of circuits are most effective in treating multi-wavelet reentry. While activation mapping to identify reentrant circuits is inviable due to the sampling requirements for MWR, we hypothesized that the distribution of circuits is dependent on electrophysiologic properties of the tissue;

areas with the shortest wavelength should have the highest probability to contain a circuit. Due to the complexity of multi-wavelet reentry, regions of tissue with shorter refractory periods will on average be excited more frequently. Therefore, identification of activation frequency should be an indirect measure of the circuit distribution. While direct measurement of tissue activation is impossible in a clinical setting, electrogram recordings provide a convoluted view of electrical events. We have demonstrated that provided sufficient spatial resolution, electrogram frequency can be used to identify circuit distribution in MWR and ablation guided by electrogram frequency maps are more effective than random ablation.

Although the spatial resolution of electrodes is attributed to manageable properties such as electrode size and configuration, the distance between a recording electrode and the tissue surface is difficult to identify clinically. Using both electrograms generated from simulated data as well as in vivo observations, we showed that the morphology of electrograms is highly sensitive to electrode height. This results in the undercounting of electrogram frequency measurements. Depending on the variation is electrode positions, changes in electrogram frequency can be on the same order as the inherent distribution of activation frequencies due to electrophysiologic heterogeneities. As a result, we sought to develop a method to determine electrode-tissue contact using the electrogram signal alone. We hypothesized that electrogram sharpness could serve as a measure for tissue contact and the difference in sharpness between two orthogonally arranged electrodes would enhance this identification. Additionally, this metric can be used to ensure orthogonality of the bipolar configuration because as the orientation approaches parallel, electrogram sharpness between the electrode pairs homogenizes. We demonstrated in both simulation and swine models that this

metric can be used to identify tissue contact and selection of frequencies based on electrogram sharpness maximizes the correlation to activation frequency.

While frequency mapping can be used to identify the distribution of circuits in multi-wavelet reentry, high-frequency sites are not unique to this mechanism. Focal drivers with fibrillatory conduction will also exhibit high-frequency regions within areas of 1:1 conduction. While ablation of focal drivers is required for successful treatment, the strategy of intervention varies depending on the driver type. Both rotor reentry and multi-wavelet reentry require the interruption of circuits with linear ablation connected to a boundary; however, termination of ectopic foci can be achieved through focal ablation. Because unnecessary ablation has been shown to have detrimental effects, a method for the identification of activation patterns would be ideal. Using simultaneous multi-site electrode recordings, we used a neural network to classify activation patterns within an area of high frequency. Using training patterns and an interpolation set generated from simulated activation, the network successfully classified 99% of patterns with enough computational efficiency to be used during clinical cases.

6.1 Suggestions for future work

The research presented provides a framework for future studies. The majority of this work is built on observations in a computational model of excitation. Ultimately, biological validation of these findings will be imperative.

Chapters 4 and 5 proposed a novel mapping technique for the treatment of multi-wavelet reentry as well as a tool to assure electrode-tissue contact. While computational findings showed promising results, it is unclear whether the simplifications

imposed create a reentrant substrate reflective of atrial fibrillation in humans. Future studies may choose either a stepwise validation of this mapping technique by evaluating its success in biophysical models and animal models of AF or take these theories straight to a clinical trial in human atrial fibrillation. While the latter can be a risky solution should these findings not translate to human AF, current treatment for patients with high levels of disease burden are less than 50% effective and therefore alternative treatments should be investigated.

Frequency mapping may also aid in another research topic arising from our lab, the fibrillogenicity index. Building on the critical mass hypothesis, this metric is used to assess the propensity of a tissue to support multi-wavelet reentry. In computational experiments, the fibrillogenicity index was found to correlate strongly with the duration of episodes of MWR and could be used to calculate titrated ablation therapy tailored to disease burden. Despite promising results during *in silico* experiments, its calculation is built on tissue parameters that are clinically impossible to measure during observation and treatment of a patient. However, we presented here that tissue frequency and, with sufficient spatial resolution, electrogram frequency correlates with tissue properties (action potential duration) and could, therefore, be used as a surrogate for unobtainable parameters to generate a clinically viable fibrillogenicity index.

The combination of frequency mapping with activation pattern classification is an exciting prospect which deserves further development. Activation pattern classification showed encouraging early findings in computational simulations. However, the activation patterns created for both training patterns and interpolation sets were ideal cases where rotors and focal sources were not impeded by fibrillatory conduction

or nearby reentrant waves. As a result, virtual electrograms generated were free from fractionation making activation time identification highly simplified. Future studies should include training and interpolation sets produced from activation patterns during fibrillation. Automated classification may prove to be unnecessary clinically as local activation mapping can reproduce excitation patterns with sufficient resolution. This, however, introduces the possibility of human bias while observing reconstructed excitation.

Comprehensive Bibliography

[1] S. M. Al-Khatib et al. "Observations on the transition from intermittent to permanent atrial fibrillation". In: *Am Heart J* 140.1 (2000), pp. 142–5.

[2] M. A. Allessie et al. "Electrophysiologic mechanisms of perpetuation of atrial fibrillation". In: *Am J Cardiol* 77.3 (1996), 10A–23A.

[3] M. A. Allessie et al. "Experimental evaluation of Moe's multiple wavelet hypothesis of atrial fibrillation". In: *Cardiac Electrophysiology and Arrhythmias*. Ed. by D. P. Zipes and J. Jalife. Grune & Stratton, 1985, pp. 265–276.

[4] Felipe Atienza et al. "Real-time Dominant Frequency Mapping and Ablation of Dominant-Frequency Sites in Atrial Fibrillation with Left-to-Right Frequency Gradients Predicts Long-Term Maintenance of Sinus Rhythm". In: *Heart Rhythm* 6.1 (2009), pp. 33–40.

[5] Troy J. Badger et al. "Evaluation of Left Atrial Lesions after Initial and Repeat Atrial Fibrillation Ablation: Lessons learned from Delayed-Enhancement MRI in Repeat Ablation Procedures". In: *Circ Arrhythm Electrophysiol* 3.3 (2010), pp. 249–259.

[6] J. Ball et al. "Atrial fibrillation: profile and burden of an evolving epidemic in the 21st century". In: *Int J Cardiol* 167.5 (2013), pp. 1807–24.

[7] E. J. Benjamin et al. "Impact of atrial fibrillation on the risk of death: the Framingham Heart Study". In: *Circulation* 98.10 (1998), pp. 946–52.

[8] B. E. Benson et al. "Mapping multi-wavelet reentry without isochrones: an electrogram-guided approach to define substrate distribution". In: *Europace* 16 Suppl 4 (2014), pp. iv102–iv109.

[9] Omer Berenfeld et al. "Spatially Distributed Dominant Excitation Frequencies Reveal Hidden Organization in Atrial Fibrillation in the Langendorff-Perfused Sheep Heart". In: *J Cardiovasc Electrophysiol* 11.8 (2000), pp. 869–879.

[10] Eric Buch et al. "Long-term clinical outcomes of focal impulse and rotor modulation for treatment of atrial fibrillation: A multicenter experience". In: *Heart Rhythm* 13.3 (2016), pp. 636–641.

[11] H. Calkins et al. "HRS/EHRA/ECAS expert Consensus Statement on catheter and surgical ablation of atrial fibrillation: recommendations for personnel, policy, procedures and follow-up. A report of the Heart Rhythm Society (HRS) Task Force on catheter and surgical ablation of atrial fibrillation". In: *Heart Rhythm* 4.6 (2007), pp. 816–61.

[12] H. Calkins et al. “Treatment of atrial fibrillation with antiarrhythmic drugs or radiofrequency ablation: two systematic literature reviews and meta-analyses”. In: *Circ Arrhythm Electrophysiol* 2.4 (2009), pp. 349–61.

[13] R. T. Carrick et al. “Ablation of multiwavelet re-entry guided by circuit-density and distribution: maximizing the probability of circuit annihilation”. In: *Circ Arrhythm Electrophysiol* 6.6 (2013), pp. 1229–35.

[14] Jay Chen et al. “Dynamics of wavelets and their role in atrial fibrillation in the isolated sheep heart”. In: *Cardiovascular Research* 48.2 (2000), pp. 220–232.

[15] M. Chen et al. “Randomized comparison between pulmonary vein antral isolation versus complex fractionated electrogram ablation for paroxysmal atrial fibrillation”. In: *J Cardiovasc Electrophysiol* 22.9 (2011), pp. 973–81.

[16] Shih-Ann Chen et al. “Radiofrequency catheter ablation of atrial fibrillation initiated by spontaneous ectopic beats”. In: *Current Cardiology Reports* 2.4 (2000), pp. 322–328.

[17] S. S. Chugh et al. “Epidemiology and natural history of atrial fibrillation: clinical implications”. In: *J Am Coll Cardiol* 37.2 (2001), pp. 371–8.

[18] S. S. Chugh et al. “Worldwide epidemiology of atrial fibrillation: a Global Burden of Disease 2010 Study”. In: *Circulation* 129.8 (2014), pp. 837–47.

[19] S. D. Corley et al. “Relationships between sinus rhythm, treatment, and survival in the Atrial Fibrillation Follow-Up Investigation of Rhythm Management (AFFIRM) Study”. In: *Circulation* 109.12 (2004), pp. 1509–13.

[20] D. D. Correa de Sa et al. “Electrogram fractionation: the relationship between spatiotemporal variation of tissue excitation and electrode spatial resolution”. In: *Circ Arrhythm Electrophysiol* 4.6 (2011), pp. 909–16.

[21] M. Courtemanche, R. J. Ramirez, and S. Nattel. “Ionic targets for drug therapy and atrial fibrillation-induced electrical remodeling: insights from a mathematical model”. In: *Cardiovasc Res* 42.2 (1999), pp. 477–89.

[22] J. L. Cox et al. “Current status of the Maze procedure for the treatment of atrial fibrillation”. In: *Semin Thorac Cardiovasc Surg* 12.1 (2000), pp. 15–9.

[23] J. L. Cox et al. “Five-year experience with the maze procedure for atrial fibrillation”. In: *Ann Thorac Surg* 56.4 (1993), pp. 814–823, 814–823.

[24] J. L. Cox et al. “The surgical treatment of atrial fibrillation. II. Intraoperative electrophysiologic mapping and description of the electrophysiologic basis of atrial flutter and atrial fibrillation”. In: *J Thorac Cardiovasc Surg* 101.3 (1991), pp. 406–26.

[25] J. L. Cox, R. B. Schuessler, and J. P. Boineau. "The surgical treatment of atrial fibrillation. I. Summary of the current concepts of the mechanisms of atrial flutter and atrial fibrillation". In: *J Thorac Cardiovasc Surg* 101.3 (1991), pp. 402–5.

[26] J. L. Cox et al. "Surgery for atrial fibrillation". In: *Semin Thorac Cardiovasc Surg* 1.1 (1989), pp. 67–73.

[27] J. L. Cox et al. "The surgical treatment of atrial fibrillation. III. Development of a definitive surgical procedure". In: *J Thorac Cardiovasc Surg* 101.4 (1991), pp. 569–83.

[28] K. S. Coyne et al. "Assessing the direct costs of treating nonvalvular atrial fibrillation in the United States". In: *Value Health* 9.5 (2006), pp. 348–56.

[29] I. Deisenhofer et al. "Does electrogram guided substrate ablation add to the success of pulmonary vein isolation in patients with paroxysmal atrial fibrillation? A prospective, randomized study". In: *J Cardiovasc Electrophysiol* 20.5 (2009), pp. 514–21.

[30] T. Deneke et al. "Histopathology of intraoperatively induced linear radiofrequency ablation lesions in patients with chronic atrial fibrillation". In: *Eur Heart J* 26.17 (2005), pp. 1797–803.

[31] Luigi Di Biase et al. "Atrial Fibrillation Ablation Strategies for Paroxysmal Patients: Randomized Comparison Between Different Techniques". In: *Circulation: Arrhythmia and Electrophysiology* 2.2 (2009), pp. 113–119.

[32] Sanjay Dixit et al. "Randomized Ablation Strategies for the Treatment of Persistent Atrial Fibrillation: RASTA Study". In: *Circulation: Arrhythmia and Electrophysiology* 5.2 (2012), pp. 287–294.

[33] Peter M Dunn. "Maimonides (1135-1204) and his philosophy of medicine". In: *Archives of Disease in Childhood - Fetal and Neonatal Edition* 79.3 (1998), F227.

[34] C. S. Elayi et al. "Ablation for longstanding permanent atrial fibrillation: results from a randomized study comparing three different strategies". In: *Heart Rhythm* 5.12 (2008), pp. 1658–64.

[35] T. Fazekas. "[The concise history of atrial fibrillation]". In: *Orvostort Kozl* 53.3-4 (2007), pp. 37–68.

[36] W. M. Feinberg et al. "Prevalence, age distribution, and gender of patients with atrial fibrillation. Analysis and implications". In: *Arch Intern Med* 155.5 (1995), pp. 469–73.

[37] G. C. Flaker et al. “Clinical and echocardiographic features of intermittent atrial fibrillation that predict recurrent atrial fibrillation. Stroke Prevention in Atrial Fibrillation (SPAF) Investigators”. In: *Am J Cardiol* 76.5 (1995), pp. 355–8.

[38] K. M. Flegel, M. J. Shipley, and G. Rose. “Risk of stroke in non-rheumatic atrial fibrillation”. In: *Lancet* 1.8532 (1987), pp. 526–9.

[39] V. Fuster et al. “ACC/AHA/ESC 2006 Guidelines for the Management of Patients with Atrial Fibrillation: a report of the American College of Cardiology/American Heart Association Task Force on Practice Guidelines and the European Society of Cardiology Committee for Practice Guidelines (Writing Committee to Revise the 2001 Guidelines for the Management of Patients With Atrial Fibrillation): developed in collaboration with the European Heart Rhythm Association and the Heart Rhythm Society”. In: *Circulation* 114.7 (2006), e257–354.

[40] F. Gaita et al. “Long-term clinical results of 2 different ablation strategies in patients with paroxysmal and persistent atrial fibrillation”. In: *Circ Arrhythm Electrophysiol* 1.4 (2008), pp. 269–75.

[41] Walter E. Garrey. *The Nature of Fibrillary Contraction of the Heart. - Its Relation to Tissue Mass and Form*. American Physiological Society, 1914, p. 18.

[42] Walter E. Garrey. “THE NATURE OF FIBRILLARY CONTRACTION OF THE HEART. - ITS RELATION TO TISSUE MASS AND FORM1”. In: *Annals of Noninvasive Electrocardiology* 3.2 (1998), pp. 163–180.

[43] A. S. Go et al. “Prevalence of diagnosed atrial fibrillation in adults: national implications for rhythm management and stroke prevention: the AnTicoagulation and Risk Factors in Atrial Fibrillation (ATRIA) Study”. In: *Jama* 285.18 (2001), pp. 2370–5.

[44] Eleonora Grandi et al. “Human Atrial Action Potential and Ca2+ Model: Sinus Rhythm and Chronic Atrial Fibrillation”. In: *Circ Res* 109.9 (2011), pp. 1055–1066.

[45] N. Habel et al. “The temporal variability of dominant frequency and complex fractionated atrial electrograms constrains the validity of sequential mapping in human atrial fibrillation”. In: *Heart Rhythm* 7.5 (2010), pp. 586–93.

[46] Michel Haïssaguerre et al. “Spontaneous Initiation of Atrial Fibrillation by Ectopic Beats Originating in the Pulmonary Veins”. In: *New England Journal of Medicine* 339.10 (1998), pp. 659–666.

[47] M. Haissaguerre et al. “Catheter ablation of long-lasting persistent atrial fibrillation: critical structures for termination”. In: *J Cardiovasc Electrophysiol* 16.11 (2005), pp. 1125–37.

[48] R. Hecht-Nielsen. “Counterpropagation networks”. In: *Appl Opt* 26.23 (1987), pp. 4979–83.

[49] J. Heeringa et al. “Prevalence, incidence and lifetime risk of atrial fibrillation: the Rotterdam study”. In: *Eur Heart J* 27.8 (2006), pp. 949–53.

[50] J. Heeringa et al. “Prevalence, incidence and lifetime risk of atrial fibrillation: the Rotterdam study”. In: *Eur Heart J* 27.8 (2006), pp. 949–53.

[51] M. Hocini et al. “Techniques, evaluation, and consequences of linear block at the left atrial roof in paroxysmal atrial fibrillation: a prospective randomized study”. In: *Circulation* 112.24 (2005), pp. 3688–96.

[52] A. L. Hodgkin and A. F. Huxley. “A quantitative description of membrane current and its application to conduction and excitation in nerve”. In: *The Journal of Physiology* 117.4 (1952), pp. 500–544.

[53] Joel Howell. “Two pioneers of electrocardiography. The correspondence between Einthoven and Lewis from 1908-1925”. In: *Medical History* 29.2 (1985), pp. 224–225.

[54] W. M. Jackman et al. “Catheter ablation of accessory atrioventricular pathways (Wolff-Parkinson-White syndrome) by radiofrequency current”. In: *N Engl J Med* 324.23 (1991), pp. 1605–11.

[55] C. T. January et al. “2014 AHA/ACC/HRS guideline for the management of patients with atrial fibrillation: executive summary: a report of the American College of Cardiology/American Heart Association Task Force on practice guidelines and the Heart Rhythm Society”. In: *Circulation* 130.23 (2014), pp. 2071–104.

[56] J.P. Joseph and K. Rajappan. “Radiofrequency ablation of cardiac arrhythmias: past, present and future”. In: *QJM* 105.4 (2012), pp. 303–314.

[57] Akira T. Kawaguchi et al. “Risks and Benefits of Combined Maze Procedure for Atrial Fibrillation Associated With Organic Heart Disease1”. In: *J Am Coll Cardiol* 28.4 (1996), pp. 985–990.

[58] C. R. Kerr et al. “Progression to chronic atrial fibrillation after the initial diagnosis of paroxysmal atrial fibrillation: results from the Canadian Registry of Atrial Fibrillation”. In: *Am Heart J* 149.3 (2005), pp. 489–96.

[59] M. H. Kim et al. “Estimation of total incremental health care costs in patients with atrial fibrillation in the United States”. In: *Circ Cardiovasc Qual Outcomes* 4.3 (2011), pp. 313–20.

[60] Teuvo Kohonen. “Self-organized formation of topologically correct feature maps”. In: *Biological Cybernetics* 43.1 (1982), pp. 59–69.

[61] Jussi T. Koivumäki, Topi Korhonen, and Pasi Tavi. “Impact of Sarcoplasmic Reticulum Calcium Release on Calcium Dynamics and Action Potential Morphology in Human Atrial Myocytes: A Computational Study”. In: *PLoS Comput Biol* 7.1 (2011), e1001067.

[62] K. T. Konings et al. “High-density mapping of electrically induced atrial fibrillation in humans”. In: *Circulation* 89.4 (1994), pp. 1665–80.

[63] Karen T.S. Konings et al. “Configuration of Unipolar Atrial Electrograms During Electrically Induced Atrial Fibrillation in Humans”. In: *Circulation* 95.5 (1997), pp. 1231–1241.

[64] Marcin Kowalski et al. “Histopathologic Characterization of Chronic Radiofrequency Ablation Lesions for Pulmonary Vein Isolation”. In: *J Am Coll Cardiol* 59.10 (2012), pp. 930–938.

[65] Koichiro Kumagai, Celeen Khrestian, and Albert L. Waldo. “Simultaneous Multisite Mapping Studies During Induced Atrial Fibrillation in the Sterile Pericarditis Model”. In: *Insights Into the Mechanism of its Maintenance* 95.2 (1997), pp. 511–521.

[66] G. Y. Lip, C. M. Brechin, and D. A. Lane. “The global burden of atrial fibrillation and stroke: a systematic review of the epidemiology of atrial fibrillation in regions outside North America and Europe”. In: *Chest* 142.6 (2012), pp. 1489–98.

[67] J. Mackenzie. “The Interpretation of the Pulsations in the Jugular Veins.” In: *Am J Med Sci* 134 (1907), pp. 12–34.

[68] A. Majeed, K. Moser, and K. Carroll. “Trends in the prevalence and management of atrial fibrillation in general practice in England and Wales, 1994-1998: analysis of data from the general practice research database”. In: *Heart* 86.3 (2001), pp. 284–8.

[69] Mary M. Maleckar et al. “Mathematical simulations of ligand-gated and cell-type specific effects on the action potential of human atrium”. In: *Progress in Biophysics and Molecular Biology* 98.2-3 (2008), pp. 161–170.

[70] G. K. Moe and J. A. Abildskov. “Atrial fibrillation as a self-sustaining arrhythmia independent of focal discharge”. In: *Am Heart J* 58.1 (1959), pp. 59–70.

[71] Gordon K. Moe, Werner C. Rheinboldt, and J. A. Abildskov. “A computer model of atrial fibrillation”. In: *Am Heart J* 67.2 (1964), pp. 200–220.

[72] Koonlawee Nademanee et al. “A new approach for catheter ablation of atrial fibrillation: mapping of the electrophysiologic substrate”. In: *J Am Coll Cardiol* 43.11 (2004), pp. 2044–2053.

[73] Sanjiv M. Narayan, David E. Krummen, and Wouter-Jan Rappel. “Clinical Mapping Approach To Diagnose Electrical Rotors and Focal Impulse Sources for Human Atrial Fibrillation”. In: *J Cardiovasc Electrophysiol* 23.5 (2012), pp. 447–454.

[74] Sanjiv M. Narayan et al. “Treatment of Atrial Fibrillation by the Ablation of Localized Sources: CONFIRM (Conventional Ablation for Atrial Fibrillation With or Without Focal Impulse and Rotor Modulation) Trial”. In: *J Am Coll Cardiol* 60.7 (2012), pp. 628–636.

[75] J. M. Nuhrich et al. “Impact of biatrial defragmentation in patients with paroxysmal atrial fibrillation: results from a randomized prospective study”. In: *Heart Rhythm* 11.9 (2014), pp. 1536–42.

[76] A. Nygren et al. “Mathematical model of an adult human atrial cell: the role of K+ currents in repolarization”. In: *Circ Res* 82.1 (1998), pp. 63–81.

[77] B. Olshansky et al. “The Atrial Fibrillation Follow-up Investigation of Rhythm Management (AFFIRM) study: approaches to control rate in atrial fibrillation”. In: *J Am Coll Cardiol* 43.7 (2004), pp. 1201–8.

[78] H. Oral et al. “A randomized assessment of the incremental role of ablation of complex fractionated atrial electrograms after antral pulmonary vein isolation for long-lasting persistent atrial fibrillation”. In: *J Am Coll Cardiol* 53.9 (2009), pp. 782–9.

[79] Hakan Oral et al. “Pulmonary Vein Isolation for Paroxysmal and Persistent Atrial Fibrillation”. In: *Circulation* 105.9 (2002), pp. 1077–1081.

[80] N. J. Patel et al. “Contemporary trends of hospitalization for atrial fibrillation in the United States, 2000 through 2010: implications for healthcare planning”. In: *Circulation* 129.23 (2014), pp. 2371–9.

[81] Sunil M. Prasad et al. “The Cox maze III procedure for atrial fibrillation: long-term efficacy in patients undergoing lone versus concomitant procedures”. In: *J Thorac Cardiovasc Surg* 126.6 (2003), pp. 1822–1827.

[82] H.P. Rang and M.M. Dale. *Pharmacology*. Churchill Livingstone, 2003.

[83] Prashanthan Sanders et al. “Spectral Analysis Identifies Sites of High-Frequency Activity Maintaining Atrial Fibrillation in Humans”. In: *Circulation* 112.6 (2005), pp. 789–797.

[84] D. Scherf, F. J. Romano, and R. Terranova. “Experimental studies on auricular flutter and auricular fibrillation”. In: *Am Heart J* 36.2 (1948), pp. 241–251.

[85] R.J Schilling et al. “Endocardial mapping of atrial fibrillation in the human right atrium using a non-contact catheter”. In: *Eur Heart J* 21.7 (2000), pp. 550–564.

[86] D. Schreiber et al. “Five-year follow-up after catheter ablation of persistent atrial fibrillation using the stepwise approach and prognostic factors for success”. In: *Circ Arrhythm Electrophysiol* 8.2 (2015), pp. 308–17.

[87] P. Sommer et al. “Successful Repeat Catheter Ablation of Recurrent Longstanding Persistent Atrial Fibrillation With Rotor Elimination as the Procedural Endpoint: A Case Series”. In: *J Cardiovasc Electrophysiol* 27.3 (2016), pp. 274–80.

[88] P. Spector. “Principles of cardiac electric propagation and their implications for re-entrant arrhythmias”. In: *Circ Arrhythm Electrophysiol* 6.3 (2013), pp. 655–61.

[89] P. Spector et al. “Meta-analysis of ablation of atrial flutter and supraventricular tachycardia”. In: *Am J Cardiol* 104.5 (2009), pp. 671–7.

[90] P. S. Spector et al. “Ablation of multi-wavelet re-entry: general principles and in silico analyses”. In: *Europace* 14 Suppl 5 (2012), pp. v106–v111.

[91] Peter S. Spector et al. “Emergence of Complex Behavior: An Interactive Model of Cardiac Excitation Provides a Powerful Tool for Understanding Electrical Propagation”. In: *Circulation: Arrhythmia and Electrophysiology* (2011).

[92] M. K. Stiles et al. “High-density mapping of atrial fibrillation in humans: relationship between high-frequency activation and electrogram fractionation”. In: *J Cardiovasc Electrophysiol* 19.12 (2008), pp. 1245–53.

[93] J. M. Stinnett-Donnelly et al. “Effects of electrode size and spacing on the resolution of intracardiac electrograms”. In: *Coron Artery Dis* 23.2 (2012), pp. 126–32.

[94] W. Stokes. *The Diseases of the heart and the aorta*. Lindsay and Blakiston, 1854.

[95] E. Svennberg et al. “Mass Screening for Untreated Atrial Fibrillation: The STROKESTOP Study”. In: *Circulation* 131.25 (2015), pp. 2176–84.

[96] N. C. Thompson et al. “Improved spatial resolution and electrogram wave direction independence with the use of an orthogonal electrode configuration”. In: *J Clin Monit Comput* 28.2 (2014), pp. 157–63.

[97] R. R. Tilz et al. “Catheter ablation of long-standing persistent atrial fibrillation: 5-year outcomes of the Hamburg Sequential Ablation Strategy”. In: *J Am Coll Cardiol* 60.19 (2012), pp. 1921–9.

[98] C. F. Tsai et al. “Initiation of atrial fibrillation by ectopic beats originating from the superior vena cava: electrophysiological characteristics and results of radiofrequency ablation”. In: *Circulation* 102.1 (2000), pp. 67–74.

[99] A. Verma et al. “Approaches to catheter ablation for persistent atrial fibrillation”. In: *N Engl J Med* 372.19 (2015), pp. 1812–22.

[100] A. Verma et al. “Relationship between complex fractionated electrograms (CFE) and dominant frequency (DF) sites and prospective assessment of adding DF-guided ablation to pulmonary vein isolation in persistent atrial fibrillation (AF)”. In: *J Cardiovasc Electrophysiol* 22.12 (2011), pp. 1309–16.

[101] Atul Verma et al. “Substrate and Trigger Ablation for Reduction of Atrial Fibrillation (STAR AF): a randomized, multicentre, international trial”. In: *Eur Heart J* 31.11 (2010), pp. 1344–1356.

[102] A. Verma et al. “A prospective, multicenter evaluation of ablating complex fractionated electrograms (CFEs) during atrial fibrillation (AF) identified by an automated mapping algorithm: acute effects on AF and efficacy as an adjuvant strategy”. In: *Heart Rhythm* 5.2 (2008), pp. 198–205.

[103] A. L. Waldo. “Management of atrial fibrillation: the need for AFFIRMative action. AFFIRM investigators. Atrial Fibrillation Follow-up Investigation of Rhythm Management”. In: *Am J Cardiol* 84.6 (1999), pp. 698–700.

[104] L. S. Wann et al. “Management of patients with atrial fibrillation (compilation of 2006 ACCF/AHA/ESC and 2011 ACCF/AHA/HRS recommendations): a report of the American College of Cardiology/American Heart Association Task Force on practice guidelines”. In: *Circulation* 127.18 (2013), pp. 1916–26.

[105] L. S. Wann et al. “2011 ACCF/AHA/HRS focused update on the management of patients with atrial fibrillation (Updating the 2006 Guideline): a report of the American College of Cardiology Foundation/American Heart Association Task Force on Practice Guidelines”. In: *J Am Coll Cardiol* 57.2 (2011), pp. 223–42.

[106] T. Weimar et al. “The cox-maze procedure for lone atrial fibrillation: a single-center experience over 2 decades”. In: *Circ Arrhythm Electrophysiol* 5.1 (2012), pp. 8–14.

[107] K.F. Wenckebach. *Arhythmia of the Heart: A Physiological and Clinical Study*. Green, 1904.

[108] M. C. Wijffels et al. “Atrial fibrillation begets atrial fibrillation. A study in awake chronically instrumented goats”. In: *Circulation* 92.7 (1995), pp. 1954–68.

[109] R. Zou et al. “Development of a computer algorithm for the detection of phase singularities and initial application to analyze simulations of atrial fibrillation”. In: *Chaos* 12.3 (2002), pp. 764–778.